Published June 1, 1995

The Voltage-activated Hydrogen Ion Conductance in Rat Alveolar Epithelial Cells Is Determined by the pH Gradient

VLADIMIR V. CHERNY,*‡ VLADISLAV S. MARKIN,‡§ and THOMAS E. DECOURSEY*

From the *Department of Molecular Biophysics and Physiology, Rush Presbyterian St. Luke's Medical Center, Chicago, Illinois 60612; ‡Frumkin Institute of Electrochemistry, Russian Academy of Sciences, Moscow, Russia; and §Department of Cell Biology and Neuroscience, University of Texas, Dallas, Texas 75235-9039

ABSTRACT Voltage-activated H^+ currents were studied in rat alveolar epithelial cells using tight-seal whole-cell voltage clamp recording and highly buffered, EGTA-containing solutions. Under these conditions, the tail current reversal potential, V_{rev}, was close to the Nernst potential, E_H, varying 52 mV/U pH over four ΔpH units (ΔpH = $pH_o - pH_i$). This result indicates that H^+ channels are extremely selective, $P_H/P_{TMA} > 10^7$, and that both internal and external pH, pH_i, and pH_o, were well controlled. The H^+ current amplitude was practically constant at any fixed ΔpH, in spite of up to 100-fold symmetrical changes in H^+ concentration. Thus, the rate-limiting step in H^+ permeation is pH independent, must be localized to the channel (entry, permeation, or exit), and is not bulk diffusion limitation. The instantaneous current-voltage relationship exhibited distinct outward rectification at symmetrical pH, suggesting asymmetry in the permeation pathway. Sigmoid activation kinetics and biexponential decay of tail currents near threshold potentials indicate that H^+ channels pass through at least two closed states before opening. The steady state H^+ conductance, g_H, as well as activation and deactivation kinetic parameters were all shifted along the voltage axis by ~40 mV/U pH by changes in pH_i or pH_o, with the exception of the fast component of tail currents which was shifted less if at all. The threshold potential at which H^+ currents were detectably activated can be described empirically as ~20–40(pH_o-pH_i) mV. If internal and external protons regulate the voltage dependence of g_H gating at separate sites, then they must be equally effective. A simpler interpretation is that gating is controlled by the pH gradient, ΔpH. We propose a simple general model to account for the observed ΔpH dependence. Protonation at an externally accessible site stabilizes the closed channel conformation. Deprotonation of this site permits a conformational change resulting in the appearance of a protonation site, possibly the same one, which is accessible via the internal solution. Protonation of the internal site stabilizes the open conformation of the channel. In summary, within

Address correspondence to Thomas E. DeCoursey, Department of Molecular Biophysics and Physiology, Rush Presbyterian St. Luke's Medical Center, 1653 West Congress Parkway, Chicago, IL 60612.

the physiological range of pH, the voltage dependence of H^+ channel gating depends on ΔpH and not on the absolute pH.

INTRODUCTION

A highly H^+-selective conductance, g_H, is activated by membrane depolarization in a number of cells. Described first in snail neurons (Thomas and Meech, 1982), its presence in mammalian cells and evidence suggesting a role in metabolic acid dissipation during phagocytosis in human neutrophils (reviewed by DeCoursey and Cherny, 1994*b*) have stimulated renewed interest in this conductance. The single-channel conductance based on noise measurements (Byerly and Suen, 1989; DeCoursey and Cherny, 1993; Bernheim, Krause, Baroffio, Hamann, Kaelin, and Bader, 1993) corresponds with a turnover rate in the range of carriers and pumps. We use the term channel because H^+ is conducted passively down its electrochemical gradient, H^+ permeation is not coupled with the movement of any other ion, ATP is not required, and the g_H displays time- and voltage-dependent gating. The mechanism of permeation probably differs significantly from that of other ion channels.

A characteristic feature of voltage-activated H^+ currents is their dependence on pH_o and pH_i. Increasing pH_o or lowering pH_i shifts the voltage dependence of activation of the g_H to more negative potentials. The magnitude of these effects varies substantially among existing studies (DeCoursey and Cherny, 1994*b*), and the relationship between pH_o, pH_i, and the voltage dependence of g_H activation has not been formally described. A significant source of variability is imperfect control of pH_i in particular, and perhaps also pH_o. It is reasonable to assume that V_{rev} reliably indicates the actual pH gradient across the membrane in the vicinity of the H^+ channel. The reversal potential, V_{rev}, of H^+ currents has been found to vary less steeply than the Nernst potential for protons, E_H, in most studies when pH_o or pH_i were changed (Mahaut-Smith, 1989*a*; DeCoursey, 1991; Demaurex, Grinstein, Jaconi, Schlegel, Lew, and Krause, 1993; Kapus, Romanek, Rotstein, and Grinstein, 1993; Bernheim et al., 1993; DeCoursey and Cherny, 1994*a*). In the present study, V_{rev} was near E_H over the range pH_o 5.5–8.0 and pH_i 5.5–7.5, demonstrating that both pH_o and pH_i were well controlled. Several factors contributed to this more consistent data. High buffer concentrations (100 mM) were used in all solutions, improving pH control and accelerating recovery of pH_i after pulses (Byerly and Moody, 1986; DeCoursey, 1991; Demaurex et al., 1993; Kapus et al., 1993). We avoided substrates for the Na^+-H^+ antiporter which indirectly inhibit H^+ currents (DeCoursey and Cherny, 1994*a*), as well as TEA^+ which alters the behavior of H^+ currents (Byerly, Meech, and Moody, 1984; Meech and Thomas, 1987; DeCoursey and Cherny, 1994*b*). Finally, we show here that addition of EGTA to the extracellular solution, even with excess Ca^{2+} to keep $[Ca^{2+}]_o$ constant, significantly enhances the g_H, with the main effect being a shift of the voltage dependence to more negative potentials, perhaps due to chelation of metal contaminants. We conclude that these conditions allow us to observe the fundamental effects of pH_o and pH_i on the g_H. We extend the description of H^+ current behavior to include both activation and deactivation kinetics over a wide range of pH_o and pH_i. The results constrain the possible types of mechanisms involved in H^+ permeation.

A remarkable pattern which emerged was that for a constant pH gradient, ΔpH =

pH_o–pH_i, most properties of the g_H were practically independent of the absolute pH, over the range pH_o 6.0–8.0 and pH_i 5.5–7.5. The H^+ current amplitude increased only twofold when the H^+ concentration was increased by 100-fold symmetrically at fixed ΔpH. Both pH_o and pH_i had similar potency in shifting the H^+ current-voltage relation and the voltage dependence of the kinetics of activation and deactivation of the g_H. The kinetic equivalence of changes in H^+ concentration and membrane potential is reminiscent of "ion well" or "access channel" models for the H^+-ATPase (Mitchell and Moyle, 1974; Läuger, 1991) or the Na^+/K^+-ATPase (Gadsby, Rakowski, and De Weer, 1993; De Weer, Rakowski, and Gadsby, 1994; Hilgemann, 1994). In contrast with these ATPases in which the ion well is accessible from only one side of the membrane, voltage-activated H^+ channels would need bilateral proton wells to account for the effects of changes in both pH_o and pH_i. The dependence of several gating properties on ΔpH led us to suggest a simple physical model in which H^+ channel gating is regulated by a site which may be protonated either from the external or internal solution, but is not accessible to both simultaneously. The accessibility of this site to protons from one or the other side of the membrane is switched by a conformational change in the channel molecule which can occur only when the site is deprotonated. Protonation of this site from the external side of the membrane stabilizes the closed channel conformation, while protonation from the inner side of the membrane stabilizes the open conformation. Calculations using this model reproduce the main features of the results.

METHODS

Cells

Type II alveolar epithelial cells were isolated from adult rats using enzyme digestion, lectin agglutination, and differential adherence, as described elsewhere (DeCoursey, Jacobs, and Silver, 1988; DeCoursey, 1990). These experiments were undertaken with the purpose of advancing knowledge. The rats were treated humanely, experienced no pain, and were killed under deep anesthesia, in compliance with law and with the NIH Guide for the Care and Use of Laboratory Animals. H^+ currents were studied in cells up to several weeks after isolation. As described previously, the properties of H^+ currents appeared to be independent of time in culture. Approximately spherical cells were selected for study.

Whole-Cell Recording

Conventional whole-cell patch clamp technique (Hamill, Marty, Neher, Sakmann, and Sigworth, 1981) was used. Experiments were done at 20°C, with the bath temperature controlled by Peltier devices and monitored continuously by a thinfilm platinum RTD (resistance temperature detector) element (Omega Engineering, Stamford, CT) immersed in the bath solution. Micropipettes were pulled in several stages using a Flaming Brown automatic pipette puller (Sutter Instruments, San Rafael, CA) from EG-6 glass (Garner Glass Co., Claremont, CA), coated with Sylgard 184 (Dow Corning Corp., Midland, MI), and heat polished to a tip resistance ranging typically between 2–6 MΩ. Electrical contact with the pipette solution was achieved by a thin sintered Ag-AgCl pellet (In Vivo Metric Systems, Healdsburg, CA) attached to a silver wire covered by a Teflon tube. A reference electrode made from a Ag-AgCl pellet was connected to the bath through an agar bridge made with Ringer's solution. The current signal from the patch clamp (List Electronic, Darmstadt, Germany) was recorded and analyzed using

an Indec Laboratory Data Acquisition and Display System (Indec Corporation, Sunnyvale, CA). Data acquisition and analysis programs were written in BASIC-23 or FORTRAN.

Solutions

Most internal and external solutions were made with 100 mM buffer and 80 mM tetramethylammonium methanesulfonate ($TMAMeSO_3$) titrated with tetramethylammonium hydroxide (TMAOH). A stock solution of $TMAMeSO_3$ was made by neutralizing TMAOH with methanesulfonic acid. External solutions also included 3 mM $CaCl_2$ and 1 mM EGTA, except for experiments described in Fig. 1, in which EGTA was omitted. The pH_o 6.0 solution included 1 mM EGTA and 2 mM $CaCl_2$, because EGTA does not buffer Ca^{2+} well at low pH (Martell and Smith, 1974; McGuigan, Lüthi, and Buri, 1991). The intent was to keep $[Ca^{2+}]_o$ constant at ~2 mM in all external solutions. Solutions at pH 5.5, 6.5, and 7.5 included 1 mM EGTA and 2 mM $MgCl_2$ and were used both in the pipette and externally. No difference was observed between H^+ currents bathed in 2 mM Ca^{2+} and 2 mM Mg^{2+}. Another solution used in many experiments at pH_i 5.5 included NMG^+ instead of TMA^+, and had 3.7 mM EGTA, 0.74 mM $CaCl_2$, and 119 mM buffer. Buffers (Sigma Chemical Co., St. Louis, MO), which were used near their pK, were: pH 5.5–6.0 MES (2-[*N*-Morpholino]ethanesulfonic acid), pH 6.5 BIS-TRIS (bis[2-Hydroxyethyl]imino-tris[hydroxymethyl]methane), pH 7.0 BES (*N,N*-bis[2-Hydroxyethyl]-2-aminoethanesulfonic acid), pH 7.5 HEPES (*N*-[2-Hydroxyethyl]piperazine-*N'*-[2-ethanesulfonic acid]), pH 8.0 TRICINE (*N*-tris[Hydroxymethyl]methylglycine), pH 9.0 CHES (2-[*N*-Cyclohexylamino]ethanesulfonic acid).

Seals were formed with Ringer's solution (160 NaCl, 4.5 KCl, 2 $CaCl_2$, 1 $MgCl_2$, 5 HEPES, pH 7.4) in the bath, and the zero current potential established after the pipette was in contact with the cell. The combined correction for the liquid junction potentials at the initial pipette/bath interface and subsequent bath/reference electrode interface derived from measured values amounts to 2–3 mV and is nearly identical for the each combination of pipette and bath solutions used. Therefore, no junction potential correction has been applied to the data. Raw data are presented without correction for leak current. To quantitate H^+ current and g_H amplitudes, a usually small linear leak conductance was subtracted based on currents during subthreshold pulses. Under certain extreme conditions, when a cell became leaky or an additional time-independent and possibly nonlinear conductance was present (e.g., at extreme positive potentials in pH 6.0//7.5 in Fig. 3 *C*), the H^+ current was defined as the time-dependent component. No other time-dependent conductances were observed consistently under the ionic conditions employed.

Special Experimental Procedures

Cells were placed initially in a bath containing Ringer's solution. H^+ currents were detectable in Ringer's solution, but increased substantially at any given potential upon changing the bath solution to a Na^+-free solution, due to the removal of indirect inhibition of H^+ currents by Na^+-H^+ antiport (DeCoursey and Cherny, 1994*a*). Over the next several minutes, the bath solution was changed repeatedly until no further increase in H^+ current during a test pulse took place. Although the behavior was fairly stable after this point, there was still a tendency as experiments progressed for the H^+ currents to become larger and to activate faster and at more negative potentials. Byerly et al. (1994) noted that H^+ current activation in snail neurons also tended to become more rapid during long experiments.

Enhancement of H^+ Currents by External EGTA

Fig. 1 illustrates that addition of EGTA to external solutions significantly enhanced H^+ currents in alveolar epithelial cells. Families of H^+ currents at pH 7.0//6.5 are plotted in a cell bathed in

solutions identical except that in Fig. 1 *A* there was 2 mM $CaCl_2$ and no EGTA, and in Fig. 1 *B* there was 3 mM $CaCl_2$ and 1 mM EGTA. Although the free $[Ca^{2+}]_o$ was about the same, the H^+ currents are obviously different. The most obvious effect of EGTA was to shift the voltage-activation curve of the g_H to more negative potentials by ~15–20 mV. The g_H was clearly activated at +20 mV in the EGTA-free solution, but at 0 mV in the EGTA-containing solution. In addition, the time course of H^+ current activation was faster at any given potential, and appeared somewhat less sigmoid in EGTA-containing solution. Similar effects were observed in ~12 cells studied systematically; and these effects were largely reversible. Because $[Ca^{2+}]_o$ and pH_o were the same, the effects of EGTA are attributable either to pharmacological effects directly on H^+ channels, or to chelation by EGTA of contaminants in our solutions originating in either the water or the chemicals. The effects of several polyvalent cations on H^+ currents are essentially identical to those of EGTA removal: smaller I_H at a given potential, slower activation, and activation at more positive potentials (Byerly et al., 1984; Barish and Baud, 1984; Meech and Thomas, 1987; Byerly and Suen, 1989; Mahaut-Smith, 1989*b*; DeCoursey, 1991; Demaurex et al., 1993; DeCoursey and Cherny, 1993; Kapus et al., 1993; Bernheim et al., 1993). Detectable effects of external Ca^{2+} on H^+ currents have been reported in myotubes (Bernheim et al., 1993), but not in snail neurons (Byerly and Suen, 1989). We saw little further effect, beyond that described in Fig. 1 for addition of EGTA, of complete removal of $[Ca^{2+}]_o$ using a

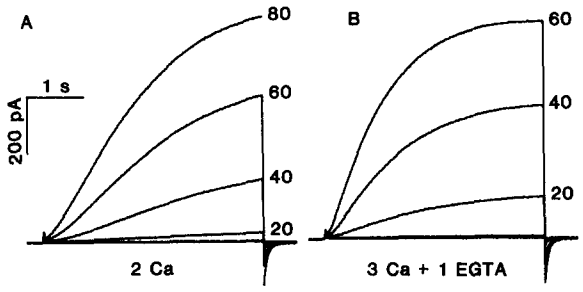

FIGURE 1. Enhancement of H^+ currents by external EGTA, in a cell at pH 7.0//6.5. Families of currents in a solution containing 2 mM $CaCl_2$ (*A*) and 3 mM $CaCl_2$ and 1 mM EGTA (*B*), with other components of solutions identical (in millimolar: 100 BES, 80 $TMAMeSO_3$, and TMAOH added to bring the pH to 7.0). Pipette contained pH_i 6.5 solution (Methods), 20°C, filter 200 Hz, pulses applied from V_{hold} −40 mV in +20-mV increments at 36-s intervals.

solution with 5 mM EGTA and no added calcium, but which included 2 mM $MgCl_2$ (data not shown). While this experiment does not rule out small effects of $[Ca^{2+}]_o$ on H^+ currents, it shows that small differences in $[Ca^{2+}]_o$ are not likely responsible for the large effects of EGTA. In subsequent experiments EGTA was included in both internal and external solutions.

RESULTS

The g_H Is Highly Selective

The selectivity of the g_H can be demonstrated by measurement of the reversal potential, V_{rev}. Examples of tail current records used to determine V_{rev} will be illustrated in Fig. 9, and are not repeated here. Fig. 2 illustrates that V_{rev} was very close to the Nernst potential for H^+, E_H, over a wide range of pH_o and pH_i, varying >200 mV over a range of pH gradients spanning 4 U. Linear regression indicates a slope of 52.4 mV/U pH (*dashed line*), close to the Nernst prediction of 58.2 mV/U pH at 20°C (*solid line*). In most previous studies, including our own studies of alveolar epithelial cells (DeCoursey, 1991), the observed V_{rev} varied in the same direction as

E_H but typically by only ~40 mV/U pH or less (Mahaut-Smith, 1989*a*; Demaurex et al., 1993; Kapus et al., 1993; Bernheim et al., 1993). The small deviation of V_{rev} from E_H in the present data could be attributable to: (*a*) finite permeability to TMA^+, corresponding with a relative permeability $P_{H^+}/P_{TMA^+} > 10^7$; (*b*) experimental error; or (*c*) a small linear H^+ leak, resulting in small differences in the actual ΔpH which in the most extreme case at pH 8.0//5.5 was <0.3 U. There is no clear indication in Fig. 2 that better agreement occurred near neutral pH_i, as had been observed in some earlier studies (Byerly et al., 1984; Demaurex et al., 1993). The present data indicate that under the conditions employed, (*a*) the g_H is extremely selective for H^+; (*b*) H^+ efflux during the prepulse of tail current measurements did not in itself significantly alter pH_i; and (*c*) over a wide range there were no significant deviations from the nominal pH of either external or internal solutions.

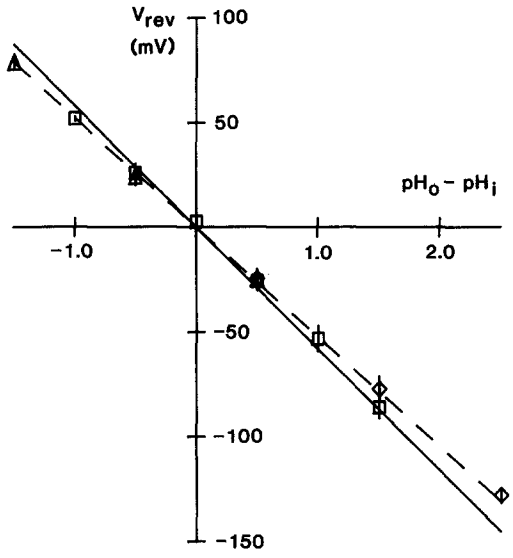

FIGURE 2. Mean reversal potentials, V_{rev}, of H^+ currents measured at a range of pH_o in cells perfused with pH_i 7.5 (△), 6.5 (□), and 5.5 (◇). (*Solid line*) E_H calculated by the Nernst equation (slope 58.2 mV/U ΔpH); (*dashed line*) linear regression on the points, with a slope of 52.4 mV/U ΔpH. Mean ± 1 SD is plotted for 2–18 determinations (total = 83) at each of the 12 different $pH_o//pH_i$ (two and three points are plotted at ΔpH = −0.5 and 0.5, respectively, but cannot be distinguished); in most cases the SD is within the point size. When multiple measurements were made at the same pH in the same cell they were averaged and included as a single datum in the mean value plotted here.

The Main Effects of pH_i and pH_o Are Shifts in the Voltage Dependence of H^+ Currents

H^+ currents appeared qualitatively similar over a wide range of pH_o and pH_i, as evident in Fig. 3. Only outward currents can be seen because the voltage-dependent activation process is shifted by pH_o or pH_i such that activation occurs only positive to E_H. The effects of pH_i and pH_o over the range explored in this figure are of approximately equivalent intensity. The threshold voltage was shifted by 40–50 mV/U pH_o (comparisons within rows), and was shifted similarly but in the opposite direction when pH_i was varied (comparisons within columns). Another way of viewing this phenomenon is to say that at a fixed pH gradient, ΔpH, the voltage-activation relationship is essentially constant. This can be seen by comparing diagonal families in Fig. 3, *B* with *F*; *A*, *E*, and *I*; *D* with *H*.

At all pH_o and pH_i studied, H^+ currents increased slowly during depolarizing pulses, and H^+ current activation was faster at more positive potentials. Two general trends apparent in Fig. 3 indicate that H^+ channel gating kinetics do not shift precisely with ΔpH. Activation appears to become progressively faster as pH_i is decreased. Within a given cell activation also appears faster as pH_o is increased. These trends were consistently observed. All of the described effects of pH_o were reversible.

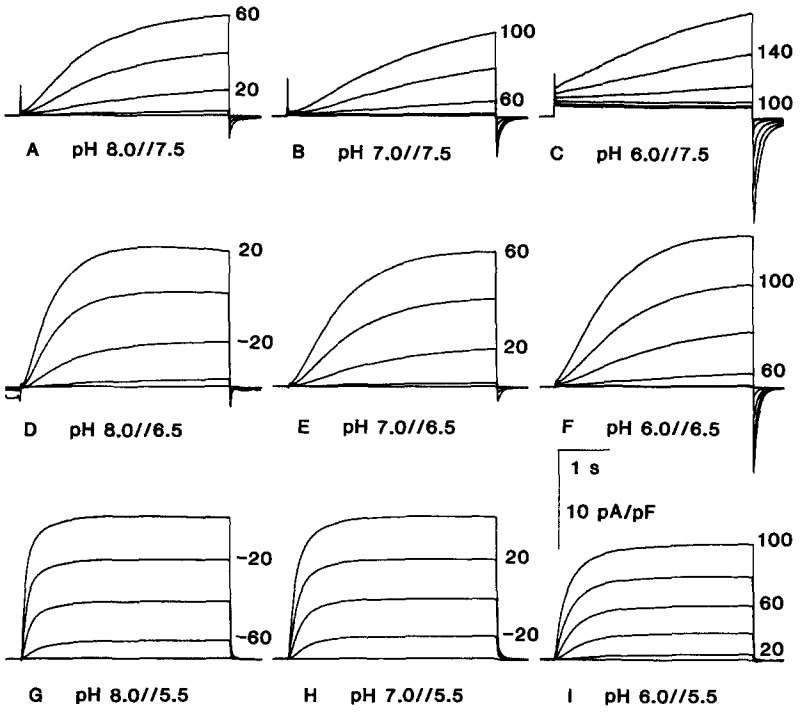

FIGURE 3. Families of H^+ currents at pH_o 8, 7, and 6 in three cells with pH_i 7.5 (*A–C*), 6.5 (*D–F*), and 5.5 (*G–I*). To facilitate comparison, the currents have been scaled according to input capacity, 30, 51, and 86 pF, respectively. All current families were obtained by applying 4-s voltage pulses in +20-mV increments at 36-s intervals. The holding potentials were set negative to the threshold for activating the g_H under the specific conditions of each measurement, and were −20 mV (*B, C, F*), −40 mV (*A, E, I*), −60 mV (*H*), or −100 mV (*D, G*). The nearly time-independent component of outward current at pH 6.0//7.5 (*C*) was also seen in some but not all other cells studied under this condition and is thus unrelated to the voltage-gated and time-dependent g_H. In each case the lowpass filter was at 200 Hz, data points were collected at 10-ms intervals.

Over the duration of individual experiments (typically up to 1–2 h), H^+ currents at a given potential often gradually became larger and activated faster. For example, the currents at pH_o 8 and 7 in the cell in Fig. 3, *G* and *H*, were recorded late in the experiment, whereas H^+ currents from an earlier run at pH_o 7 (data not shown) were smaller and more closely resembled the currents at pH_o 6 (Fig. 3 *I*), also recorded

early in the experiment. We therefore placed more emphasis on measurements taken temporally close to each other in a given experiment, and periodically returned to the same solution to monitor any slow changes in the g_H.

The Voltage Dependence of H^+ Current Activation Depends on pH_i and pH_o but the Effect of pH_o Saturates

Average values of the H^+ current, I_H, at the end of pulses like those in Fig. 3 are plotted for a number of cells in Fig. 4. At any given pH_o the average I_H-V relationship was shifted by ~40 mV/U pH in cells studied at pH_i 5.5, 6.5, or 7.5 (Fig. 4, *A–C*). The I_H-V relationship appears to become less steep at pH_i 7.5 in each case. However, the significance of this result is complicated by the fact that the driving force (V–V_{rev}) is smallest at high pH_i because V_{rev} is very near the threshold for activation of H^+ currents, whereas at lower pH_i there is a larger separation between V_{rev} and threshold.

Fig. 4 *D* illustrates average I_H-V relationships from cells studied at pH_i 7.5 and four different pH_o. Between pH_o 6 and 8, the I_H-V relationships shifted essentially identically as when pH_i was varied, namely by ~40 mV/U pH. The shift between pH_o 8 and 9 was distinctly smaller. This result may indicate the approach of pH_o to the pKa of a protonation site which regulates the voltage dependence of g_H gating (see Theoretical section).

The data at different pH_o and pH_i are superimposed in Fig. 4 *E* to illustrate that at any given ΔpH the I_H-V relationship was nearly identical. Within the scatter of the data, the voltage dependence of H^+ current activation appears to depend only on ΔpH. In other words, pH_o and pH_i are equally effective in regulating the voltage dependence of g_H activation. Comparing the effects of pH_i at a fixed ΔpH, rather than at a constant pH_o as has been done in previous studies, avoids complications due to the varying driving force. Although the H^+ currents at pH_i 7.5 (▲) for large depolarizations tended to be smaller than at lower pH_i, the largest difference at any potential and any ΔpH was <twofold, and in no case was the difference significant ($P > 0.05$). Considering that the concentration of H^+ is 100 times smaller at pH_i 7.5 than 5.5, the H^+ current amplitudes were remarkably similar.

Instantaneous Current-Voltage Relationship

Although single H^+ channel currents are too small to have been observed directly, open channel rectification can be explored by measuring the instantaneous current-voltage (I_0-V) relationship. As illustrated in Fig. 5 *A*, a prepulse which activated the g_H was followed by a test pulses to various potentials. At negative potentials the "tail" current decays essentially completely whereas at large positive test potentials further activation occurs during the test pulse. Because the same number of H^+ channels is open at the end of each identical prepulse, the instantaneous current, I_0, measured at the beginning of the test pulse reflects the ability of these channels to conduct current at that potential. The I_0-V relationship in a cell studied in symmetrical pH 6.5//6.5 is plotted in Fig. 5 *B*. A simple resistor would produce an ohmic, or linear, I_0-V relationship, as would be predicted by the GHK current equation. Instead, there was distinct outward rectification, such that the slope conductance for large outward currents was about twice that for inward currents. Moderate outward rectification was

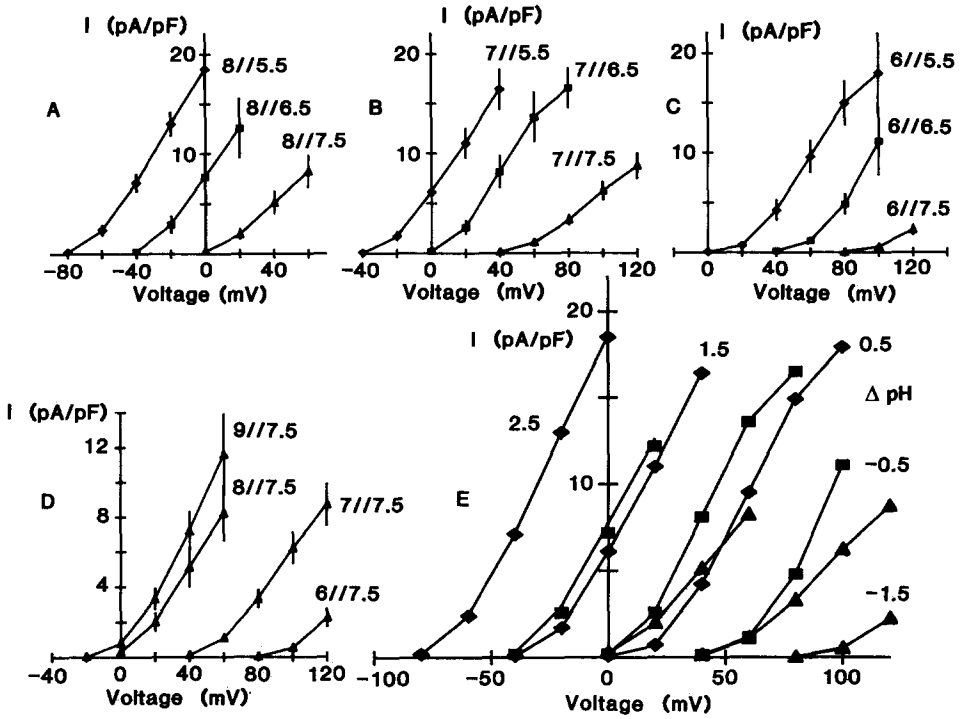

FIGURE 4. The effects of pH_i and pH_o on the H^+ current, I_H, (mean ± SEM) measured at the end of 4-s pulses in families of pulses like those in Fig. 3. In each part, pH_i is indicated by symbol shape, pH_i 5.5 = ◆, pH_i 6.5 = ■, and pH_i 7.5 = ▲. Note that although the voltage spans the same 160-mV range in each part *A–D*, the absolute potentials are different. Effect of pH_i on H^+ currents is compared in cells with pH_o 8.0 (*A*), pH_o 7.0 (*B*), and pH_o 6.0 (*C*). Numbers of cells (*n*) for *A*: pH 8//5.5, n = 4–6, pH 8//6.5, n = 5, pH 8//7.5, n = 9, for *B*: pH 7//5.5, n = 5–10, pH 7//6.5, n = 6–9, pH 7//7.5, n = 5–16, for *C*: pH 6//5.5, n = 3–5, pH 6//6.5, n = 3–5, pH 6//7.5, n = 5–6. At pH 6.0//7.5 only two cells (one of which is illustrated in Fig. 3 *C*) survived pulses up to +140 mV, thus this extreme voltage range is not represented in the mean data. (*D*) Effect of pH_o on average I_H for cells studied with pH_i 7.5, labeled according to pH_o, with n = 5–6 at pH_o 9, and other pH_o data as plotted in *A–C*. Note that the shift between pH_o 8 and 9 is smaller than at lower pH_o. (*E*) The data from parts *A–C* are superimposed on the same graph to show the similarity of I_H at each ΔpH. No significant difference exists between I_H data at any ΔpH and voltage ($P > 0.05$).

observed in this and other cells studied at several ΔpH from −0.5 to 1.5 (at ΔpH > 1.5 the amplitude of inward tail currents could not be reliably determined). Rectification appeared to be more pronounced at larger ΔpH.

The G_H-V Relationship

The chord conductance, g_H, at the end of depolarizing pulses was calculated using V_{rev} values measured in each solution in each cell. This procedure corrects the I_H data for variations in the driving force for H^+ currents. In Fig. 6, the average specific conductance, G_H, normalized to the input capacity in each cell is plotted. Over the

range of pH studied, G_H approached similar values at large depolarizations above V_{rev}. Remarkably, G_H was practically the same at any ΔpH regardless of absolute pH. As for I_H, the G_H values for large depolarizations were slightly smaller at pH_i 7.5 than at lower pH_i, however this difference was never more than a factor of two, and was not statistically significant ($P > 0.05$). The position of the G_H-V relationship on the voltage axis evidently is determined by ΔpH just as was the I_H-V relationship, shifting ~40 mV/U ΔpH whether pH_o or pH_i was changed. If pH_o and pH_i exert independent regulatory control via separate protonation sites, then these sites must be considered equally effective in setting the position of the G_H-V relationship.

The voltage dependence of ion channel gating in general can be evaluated from the steady state conductance-voltage relationship. The conductance will be propor-

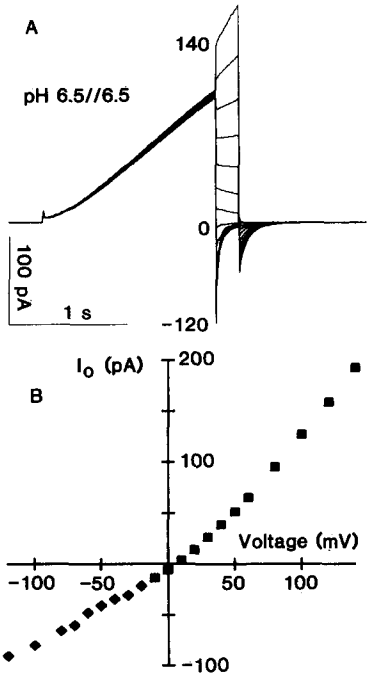

FIGURE 5. (*A*) Measurement of the instantaneous current-voltage relationship in a cell studied at pH 6.5//6.5. A prepulse to +110 mV was applied from V_{hold} −40 mV, followed by brief test pulses to a range of potentials, shown in 20-mV increments from −120 to +140 mV. (*B*) Outward rectification of the instantaneous current-voltage relationship in this experiment. The current at the beginning of the test pulse is plotted (■) where time-dependent changes were relatively slow. At negative potentials, a single exponential was fitted to the decaying tail current and extrapolated back to the start of the pulse to establish the instantaneous current (◆). Note that at symmetrical pH the slope conductance for large outward currents is ~twofold greater than for inward currents.

tional to the number of open channels, provided that the instantaneous current-voltage relationship is linear. It has been noted that g_H-V relationships in alveolar epithelial cells (DeCoursey and Cherny, 1994*a*) and in snail neurons (Byerly et al., 1984) are fitted only approximately by a Boltzmann function:

$$g_H(V) = g_{H,max}/(1 + \exp[(V_{1/2}-V)/V_{slope}]), \quad (1)$$

where $g_{H,max}$ is the limiting conductance, $V_{1/2}$ is the half-activation potential, and V_{slope} is a slope factor. Fig. 7 *A* illustrates the best fit of Eq. 1 to g_H-V data at four pH_o in a cell perfused with pH_i 6.5. The slope factors, V_{slope}, were similar, 10–14 mV, and the midpoints were shifted by ~50 mV/U pH_o. Although the g_H data are reasonably well fitted by the curves, the deviations (namely the steeper rise near threshold, and

lack of convincing saturation) were consistently observed. Furthermore, different parameters were obtained from the fits if more or fewer data points were included. The fit of g_H-V data to a Hodgkin-Huxley parameter raised to an exponent (2 or 4) was statistically better (lower Hamilton's R) but exhibited the same consistent deviation.

Correcting the data for instantaneous rectification only slightly improved the fit to Eq. 1 (Fig. 7 *B*). Each I_H value was divided by I_0 measured at the same potential. Thus evaluated in the same solutions and cells, the g_H-V relationship was steepened slightly, with $V_{slope} \sim 1$ mV smaller, and the midpoints, $V_{1/2}$, a few mV more negative.

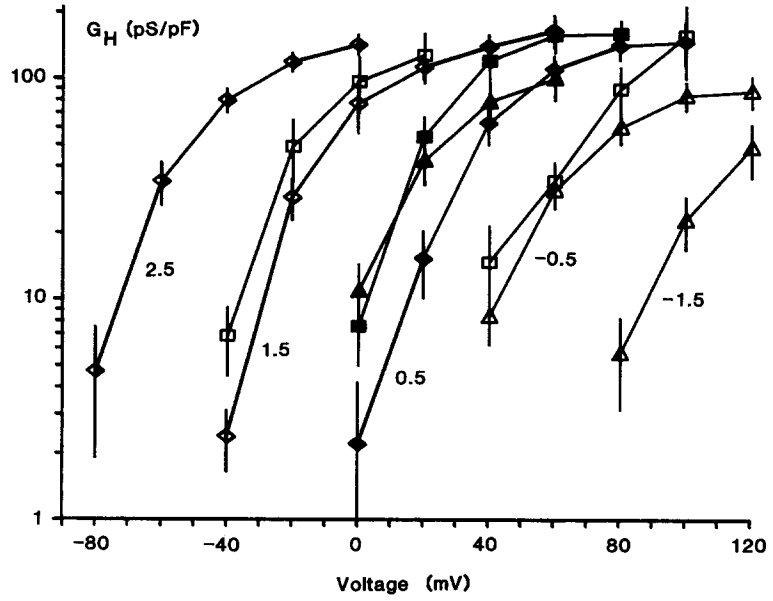

FIGURE 6. Average chord conductance G_H (normalized by dividing g_H by the input capacity) for a range of pH_o and pH_i. Mean ± SEM is plotted with numbers of experiments given in Fig. 4, with the same meaning for symbol shape, pH_i 5.5 = ◇, pH_i 6.5 = □, and pH_i 7.5 = △. Similar shading of symbols indicates the same ΔpH, which is indicated on the figure near each set of symbols. Only two pairs of data points are significantly different at $P < 0.05$; ◇ < □ at −40 mV and ◆ < ■ at +20 mV.

Several other complications (H^+ depletion/accumulation phenomena, slow gating kinetics) limit the quantitative usefulness of g_H-V data (discussed in DeCoursey and Cherny, 1994*a*,*b*). Nevertheless, the slope of the P_{open}-V relationship is likely closer to values obtained by this procedure. We did not observe any consistent pattern of effects of pH on V_{slope}, but the arbitrariness of the fit weakens this result.

Activation Kinetics: Maximum Rate-of-Rise of H^+ Currents (I'_H)

The time course of activation, or turn on, of H^+ currents in most mammalian cells is distinctly sigmoid (DeCoursey and Cherny, 1994*b*). In human neutrophils a Hodgkin-

Huxley parameter raised to the 1.5–2.0 power gave a reasonable fit to the rising phase of H^+ currents (DeCoursey and Cherny, 1993). In alveolar epithelial cells, the time course of H^+ currents could not be fitted with a gating parameter raised to any fixed exponent. The optimal exponent in a given cell varied from ~1.1 to 2.0 at various potentials, or when pH_o was varied. For this and other reasons, we used the maximum rate-of-rise of H^+ currents, I'_H, as an indicator of activation kinetics. Fig. 8 *A* illustrates the average I'_H-V relationship at four pH_o in cells perfused with pH_i 7.5 solution. Over the range pH_o 6–8 I'_H was shifted by ~45 mV/U pH_o, slightly larger than the shifts of I_H-V and g_H-V. There was a smaller shift between pH_o 8 and 9 of

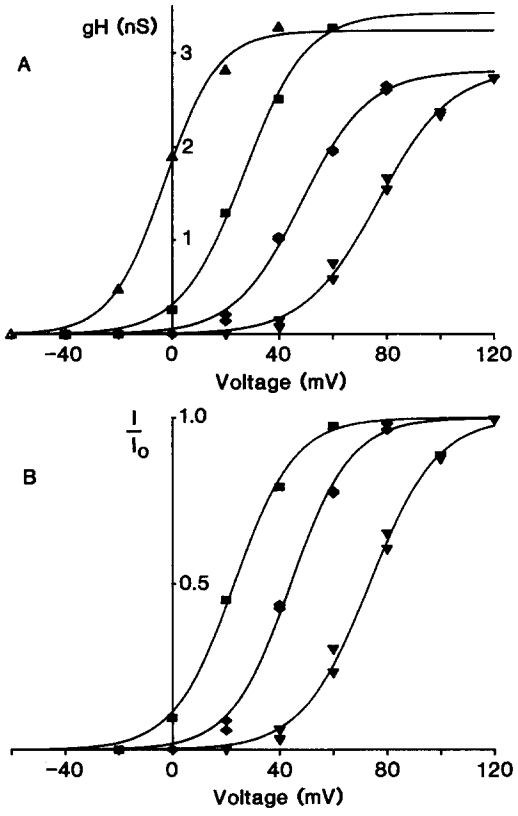

FIGURE 7. (*A*) Chord conductance-voltage relationships in a cell at pH_i 6.5 at four pH_o. Chord conductance was calculated from the H^+ current at the end of 4-s pulses, using V_{rev} measured in this cell in each solution. The best-fitting Boltzmann function (Eq. 1) is plotted for each data set, with parameters at (▲) pH_o 8.0, (■) pH_o 7.5, (◆) pH_o 7.0, and (▼) pH_o 6.5, respectively: $V_{1/2}$ = −2.8, 26.8, 48.3, and 76.6 mV; V_{slope} = 9.95, 11.72, 12.43, and 13.51 mV; $g_{H,max}$ = 3.24, 3.43, 2.81, and 2.82 nS.

(*B*) The same data as in *A*, after correction for instantaneous rectification, omitting pH_o 8.0, for which I_0-V data were not obtained. The I_H data were divided by the instantaneous current measured at each potential after a prepulse, as illustrated in Fig. 5 *A*, and then normalized to the fitted maximum value. Fitted parameters at (■) pH_o 7.5, (◆) pH_o 7.0, and (▼) pH_o 6.5 are: $V_{1/2}$ = 23.1, 44.3, 73.5 mV; V_{slope} = 11.32, 11.23, 12.6 mV. The correction steepened each curve slightly.

~20 mV. This result is analogous to the saturation of the effect of pH_o on I_H-V relationships in Fig. 4 *D*. The I_H parameter is a mixture of activation kinetics, driving force (V-V_{rev}), and open probability. When pH_o was changed from 8 to 9, E_H was shifted much more than was the voltage dependence of activation. (V_{rev} could not be accurately estimated in experiments at pH 9.0//7.5 because inward tail currents were not convincingly resolved, but must have been more negative than −60 mV, at which potential tail currents in three cells were still detectably outward.) The substantially increased driving force at pH_o 9 for a given level of activation results in a vertical as well as a horizontal shift of the I'_H-V relationship.

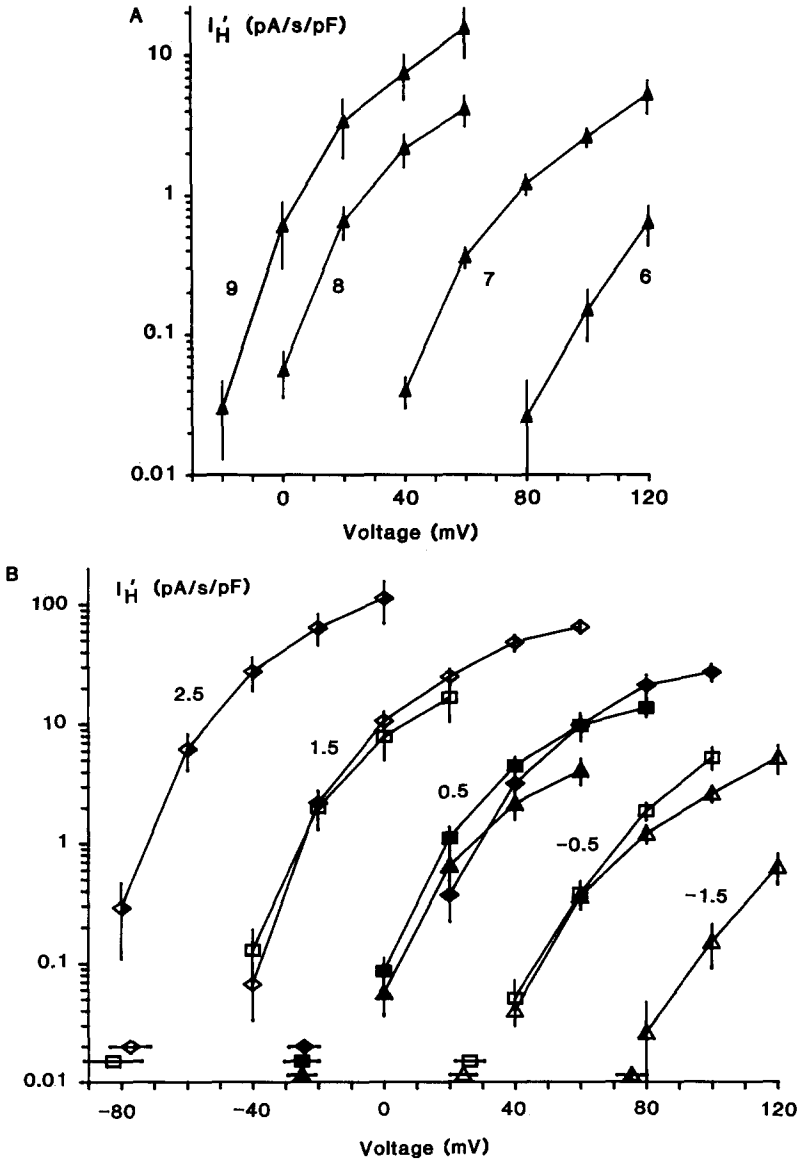

FIGURE 8. (*A*) Dependence of the maximum rate-of-rise of H^+ currents, I'_H, on pH_o (labels on the graph) in cells studied with pH_i 7.5. The values were normalized according to input capacity of each cell and then averaged. Numbers of experiments are given in Fig. 4 *D*.

(*B*) Dependence of maximum rate-of-rise of H^+ currents, I'_H, on ΔpH. Symbol shape indicates pH_i as in other figures, pH_i 5.5 = ◇, pH_i 6.5 = □, and pH_i 7.5 = △, shading indicates ΔpH as labeled near each set of data points. Mean ± SEM are plotted for the numbers of experiments in Fig. 4. The symbols plotted near the abscissae show the mean V_{rev} ± SD measured in the same cells for which I'_H data are plotted, using matching symbols. Note that V_{rev} is near the threshold for activation of H^+ currents at ΔpH = −1.5 (pH 6.0//7.5) and becomes progressively more negative than threshold as ΔpH increases. For ΔpH = 2.5 (pH 8.0//5.5) V_{rev} was −128 ± 3.2 mV (n = 3) and is not plotted.

Average I'_H-V relationships at pH_o 6.0–8.0 and pH_i 5.5–7.5 are plotted in Fig. 8 *B*. The most striking result is that at any given ΔpH (indicated on the figure), I'_H was essentially identical, that is, independent of the absolute pH. The magnitude of the voltage shift with ΔpH appears to be 45–50 mV/U ΔpH, slightly larger than the 40 mV observed for I_H and g_H, but part of this difference can be ascribed to progressive changes in driving force, as discussed for Fig. 8 *A*. The mean V_{rev} measured in those cells for which data are plotted in Fig. 8 *B* are indicated near the abscissae. Because V_{rev} changed by ~52 mV/U ΔpH (Fig. 2), whereas the voltage dependence of g_H activation shifted by only ~40 mV, the driving force for a given level of activation increased progressively as ΔpH was increased. Thus, V_{rev} was nearly at the threshold for activating H^+ currents at pH 6.0//7.5, but was ~50 mV negative to threshold at pH 8.0//5.5 Due in part to this difference, at high ΔpH the values of I'_H are larger for a given level of activation of the g_H, and thus there is a tendency for the I'_H-V curves to shift upward as well as to more negative potentials as ΔpH is increased. This situation makes it difficult to make quantitative comparisons of the effects of either pH_o or pH_i individually, but do not affect comparisons when both are changed symmetrically, i.e. when ΔpH is held constant. As with the G_H-V relationships, at fixed ΔpH there was a only a small reduction of I'_H when the H^+ concentration was reduced symmetrically by 100-fold. The similarity of I'_H at any fixed ΔpH at various absolute pH is more striking than are any subtle differences.

Deactivation Kinetics

After H^+ current has been elicited by a depolarizing pulse, repolarization results in a tail current, which decays with a time course reflecting the rate that H^+ channels close at that potential. Examples of tail currents at pH_o 7.5, 6.5, and 5.5 in a cell perfused with pH_i 6.5 are illustrated in Fig. 9, *A–C*. Tail currents after depolarizing prepulses usually decayed exponentially at voltages around and more negative than V_{rev}. Like nearly all voltage-gated ion channels, H^+ channels close more rapidly at more negative potentials. At more positive voltages approaching the threshold for activating H^+ currents, a slower component of current decay became obvious. The presence of two distinct kinetic components in the tail currents was most obvious at a high ΔpH, for example at pH 7.5//6.5 in Fig. 9 *A*, and was less pronounced at low ΔpH, as at pH 5.5//6.5 in Fig. 9 *C*; however, the decay was still biexponential. This pattern suggests that the two kinetic components may not shift equally with changes in ΔpH.

Tail currents were fitted with a single exponential function and the time constant of decay, τ_{tail}, plotted at several pH_o and pH_i in Fig. 9 *D*. The average τ_{tail}-V relationship was approximately linear on semilog axes, consistent with an exponential voltage dependence, especially at large negative potentials. At ΔpH = 1.5 the averaged τ_{tail} changed e-fold in 50–55 mV. This slope is flatter than observed in many individual cells, ~35–40 mV/e-fold change, perhaps due in part to smearing of the data by averaging. At more positive potentials, near threshold potentials for activating the g_H, τ_{tail} appeared to become more steeply voltage dependent. However, this voltage range coincides with the appearance of the slower component of current decay, thus the apparent increase in steepness may reflect contamination by the slower component. Fig. 9 *D* shows that τ_{tail} was essentially the same at a given ΔpH

Published June 1, 1995

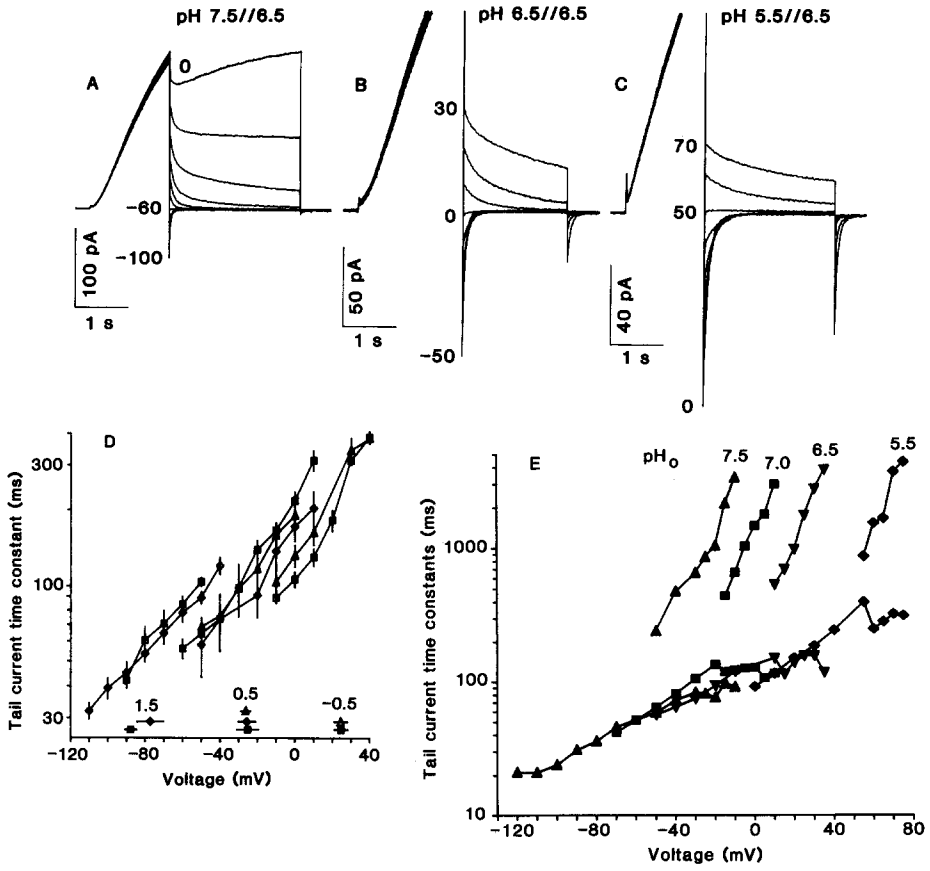

FIGURE 9. Tail currents in a cell at pH_i 6.5, at three different pH_o. (*A*) Tail currents at pH 7.5//6.5. V_{hold} was −60 mV, a 1.5-s prepulse to +10 mV was followed by 2.5-s test pulses to −100 mV through 0 mV in 10-mV increments. Note that at more positive potentials distinct rapid and slow decay phases are apparent, and that at 0 mV the rapid decay of H^+ current is followed by a slower rising phase. (*B*) Tails at symmetrical pH 6.5//6.5 from V_{hold}-40 mV, with 2-s prepulses to +70 mV followed by 2-s test pulses to −50 through +30 mV. (*C*) Tails at pH 5.5//6.5 from V_{hold} −20 mV with 1.5-s prepulses to +120 mV followed by 2.5-s test pulses to 0 mV through +70 mV.

(*D*) Voltage dependence of tail current time constants, τ_{tail}, at three different ΔpH. Tail currents like those in *A–C* were fitted by a single exponential, and the mean ± SEM is plotted. At the more positive potentials of each data set, when a slower component of decay became evident, the fit was biased toward the faster component, and when the slower component became large data were excluded. Shape of symbols indicates pH_i (pH_i 5.5 = ◇, pH_i 6.5 = □, and pH_i 7.5 = △), and shading of symbols indicates the ΔpH as indicated on the graph. Data points just above the abscissae indicate mean ± SD V_{rev} observed in the same cells in which τ_{tail} was measured. Numbers of experiments for ΔpH = 1.5 (pH 7.0//5.5, n = 4–10; pH 8.0//6.5, n = 3), for ΔpH = 0.5 (pH 6.0//5.5, n = 3–5; pH 7.0//6.5, n = 3–9; pH 8.0//7.5, n = 4–6), and for ΔpH = −0.5 (pH 6.0//6.5, n = 4; pH 7.0//7.5, n = 4–8).

(*E*) Voltage dependence of fast (τ_{fast}) and slow (τ_{slow}) components of tail currents in the same cell as in parts *A–C*, at several pH_o as indicated on the figure. Tail currents were fitted by a single exponential at relatively negative potentials, or to the sum of two exponentials at more positive potentials. Separate lines connect τ_{fast} (or the single exponential τ_{tail} in the more negative range) and τ_{slow} for each pH_o studied. The slower component was more steeply voltage- and pH_o-dependent than τ_{fast}. Note that the τ axis spans a wider range than in *D*.

regardless of the absolute pH. H^+ current deactivation kinetics thus exhibited ΔpH dependence, as did g_H, I_H, and I'_H. However, the shift of the average τ_{tail}-V relationships with ΔpH was at most only ~20 mV/U ΔpH, much less than that of the other parameters.

Tail currents in several experiments were analyzed further by double exponential fits at relatively positive potentials (Fig. 9 *E*). The time constant of the faster component, τ_{fast}, corresponded with τ_{tail} values for the single exponential decay at potentials negative to V_{rev} and was only weakly voltage dependent. In contrast, the time constant of the slower component, τ_{slow}, was steeply voltage dependent, changing e-fold/8–15 mV, and shifted by ~40 mV/U pH_o. In the experiment illustrated in Fig. 9 *E*, pH_o over a wide range did not convincingly alter τ_{fast} at all. In view of this result, we cannot rule out the possibility that the faster component may be completely insensitive to pH_o, and that the small shifts in the averaged τ_{tail} data in Fig. 9 *D* are due to contamination of the fit by the strongly pH dependent slower component. τ_{slow} ranged up to several seconds, about an order-of-magnitude slower than τ_{fast}. The slower component thus appears to be related kinetically to the activation process, in that both are slow and shift ~40 mV/U pH_o when pH_o is varied.

THEORETICAL

Hypotheses

It seems reasonable to suggest that the conductance of the open H^+ channel is independent of the proton concentration at either side of membrane (Fig. 6) and of membrane voltage (ignoring for now the rectification in Fig. 5 *B*). Then all pH and voltage dependencies should be ascribed to the channel open probability alone. There are closed and open conformations of the channel, and protons outside the cell stabilize the closed state while protons in the cell stabilize the open state. If the ratio of the open-state probability to the closed one were proportional to $[H]_{in}/[H]_{out}$, the open probability could depend on ΔpH only. One tentative modeling idea that could explain this observation incorporates the following hypotheses: (*a*) the conductance of the open channel is independent of proton concentration; (*b*) the transition between open and closed states of the channel is regulated by proton adsorption at either side of membrane to a site associated with the channel; (*c*) this regulatory site is accessible from only one side of membrane at a time; (*d*) the regulatory site can change orientation (accessibility) in deprontonated form only; and (*e*) the orientation of the regulatory site and/or proton adsorption is voltage dependent.

The "Butterfly" Model

Let us visualize the voltage-activated proton-regulated H^+ channel as a multimeric structure consisting of j protomers, or wings (Fig. 10 *A*). The wings can move independently of each other and only if they are not protonated. When they are protonated, they are immobilized in the corresponding position. The channel conducts only when all wings are down and protonated (state 4). As follows from the analysis below, we have to consider at least two ($j = 2$) protomers or wings that can move up to the horizontal position and down to the vertical position where they can

form a conducting pathway or a pore. Fig. 10, *B* and *C*, illustrate alternative depictions of the proposed gating mechanism, all of which are mathematically equivalent. Some properties may be more readily visualized using one picture or another. For convenience, we will describe the model using the image in Fig. 10 *A*.

The minimal state diagram for each wing includes the four states shown in Fig. 10 with corresponding rate constants. The rates of transitions of a single wing between

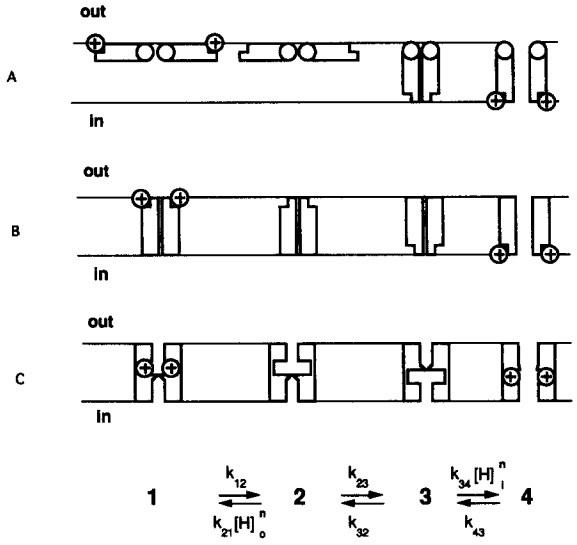

FIGURE 10. Physical representations of the model defined by the state diagram and rate constants. The mechanism can be envisioned as (*A*) a "butterfly" in which the protonation site on each channel protomer or "wing" moves across the membrane; (*B*) distinct external and internal sites which when protonated allosterically prevent protonation at the opposite site; (*C*) a protonation site in a proton well whose accessibility depends on a small conformational change, or other variants not illustrated. The diagram in *C* would be a proton carrier (Läuger, 1986) if the conformational change occurred in the protonated state, i.e., if there were direct transitions between states 1 and 4 and if no conducting pore were formed. In each case, the formation of a conducting H^+ channel requires a conformational change in each channel protomer which can occur only when the regulatory site is deprotonated. Thus, the closed channel conformation is stabilized by external protons, and the open configuration is stabilized by internal protonation of the same site, which is possible only after the conformational change exposes the protonation site to the internal solution. The open channel probability is therefore increased by high pH_o or low pH_i. The voltage dependence of H^+ channel gating could arise either from voltage-dependent binding/unbinding of protons to the regulatory protonation site, or from a voltage-dependent conformational change, or some combination of the two. In the version of the model used for the calculations in Figs. 11–13, we assigned all of the voltage dependence to proton binding, so that the regulatory sites behave like "proton wells" as postulated for the proton channel of H^+-ATPases (Mitchell and Moyle, 1974; Läuger, 1991). All calculations were done using the following parameters: $\delta_{in} = \delta_{out} = 0.71$, $K_W = 10$, $m = 0$, $n = 1.5$, $j = 2$, $k_{12} = 1{,}000\ s^{-1}$, $k_{32} = 10^6\ s^{-1}$, $k_{43,fast} = 3\ s^{-1}$, $k_{43,slow} = 0.05\ s^{-1}$, $pK_{in} = pK_{out} = 8.5$.

different states r_{ik} depend on proton concentrations inside and outside the cell and on membrane potential. The transition of a single wing from state 2 to state 1 involves adsorption of n protons, and hence, it is pH dependent. If H^+ adsorption occurs at the surface of membrane, it might not be sensitive to membrane potential. But if the adsorption site is immersed in a proton well, then the protons experience the effect of some fraction of the membrane potential. For external protons we

denote this fraction δ_{out} and for internal protons δ_{in}. In this case channel opening becomes voltage dependent.

Another kind of voltage dependence can arise if the wings are charged, i.e., if the transition from state 2 to state 3 involves the movement of effective charge me_0. In a general case, both proton wells and charged wings can contribute to the voltage dependence of the proton channel.

Predicting steady state behavior demands fewer assumptions from the model than does kinetics, therefore, we first present the steady state dependencies and only afterwards address the kinetic data. The equations describing this model are derived in the Appendix and their solution provides the steady state conductance. In the general case, even the steady state conductance is a rather involved function but by making reasonable assumptions described in the Appendix, this conductance reduces to the form of a Boltzmann function of potential:

$$g_H = \frac{g_{H,max}}{1 + \exp\left[(V_{1/2} - V)/V_{slope}\right]} \quad (1)$$

with half-activation potential:

$$V_{1/2} = \frac{k_B T[0.881 + \ln K_w + 2.3n(\Delta pK - \Delta pH)]}{e_0[m + n(\delta_{in} + \delta_{out})]} \quad (2)$$

and slope factor:

$$V_{slope} = \frac{k_B T}{1.17 e_0[m + n(\delta_{in} + \delta_{out})]} \quad (3)$$

where k_B is Boltzmann's constant, T is the absolute temperature, and e_0 is the elementary charge. As one can see from Eq. 2, in this approximation the conductance depends only on ΔpH and does not depend on the magnitude of pH at each side. When ΔpH is changed the half activation potential shifts as:

$$\Delta V_{1/2} = \frac{-2.3nk_B T}{e_0[m + n(\delta_{in} + \delta_{out})]} \Delta pH = -2.7nV_{slope}\Delta pH \quad (4)$$

Kinetic processes in this model are described by more complicated equations and in practice should be found numerically, if the parameters of the model are known.

Parameters of the Model

Comparing the steady state predictions of the theory with experimental observations, we can find the most important parameters of the model: m, n, δ_{in}, and δ_{out}. To a first approximation, the experimental dependence of the g_H on potential (Fig. 7 *B*) can be described by a Boltzmannian with a slope factor V_{slope} = 10 mV. When ΔpH is changed the g_H-V curve shifts ~ −40 mV/U pH. We can conclude from Eq. 4 that n = 1.5, so that the whole complex is regulated by the adsorption of three protons.

From Eq. 3 we find that:

$$m + n(\delta_{in} + \delta_{out}) = 2.14. \quad (5)$$

There are two possible sources of voltage dependence of channel opening: displace-

ment of the wing charge me_0 accompanying wing movement (the transition between states 2 and 3) and/or proton adsorption in wells where the protons "feel" some fraction of the membrane potential. As one can see from the preceding equations, both charges enter the equations in a similar manner and in that sense they are almost indistinguishable in steady state measurements. Nevertheless, we can find characteristic parameters for both cases.

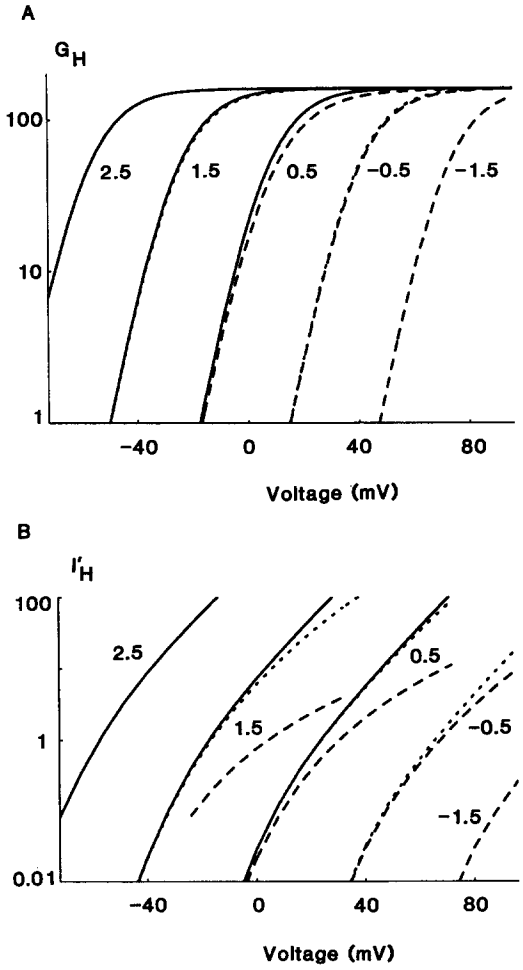

FIGURE 11. (*A*) Steady state g_H calculated using the model parameters as in Fig. 10, for conditions like those in Fig. 6. (*Solid curves*) pH_i 5.5; (*dotted curves*) pH_i 6.5; and (*dashed curves*) pH_i 7.5 curves are labeled with ΔpH. Note that these are true steady state g_H, whereas the data were sampled at the end of 4-s pulses, which in many cases clearly was before steady state level had been achieved (see text for further discussion). Assumed $g_{H,max}$ was 140 pS/pF.

(*B*) Simulated $I'_H V$ relationships calculated for conditions like those in Fig. 8 *B*, with curves coded as in *A*. Note that pH 9.0//7.5 is plotted here but not in Fig. 8 *B*, to show the saturation of the effect of the external protonation site at high pH_o as was illustrated in Fig. 8 *A*. The calculated I'_H is in arbitrary units.

Charged wings. Suppose that protons adsorb at the membrane surfaces and $\delta_{in} = \delta_{out} = 0$. Then the whole voltage dependence will originate from the movement of the wings and from Eq. 5, $m = 2.14$, i.e., the effective charge of a wing is 2.14 e_0. In this case the model successfully reproduces experimental observations on V_{slope} and on the shift of the g_H-V curve with changes in ΔpH. Over a broad range of pH the conductance depends on ΔpH only rather than an absolute value of pH. When pH approaches the pK of the regulatory site, the conductance is described by the general

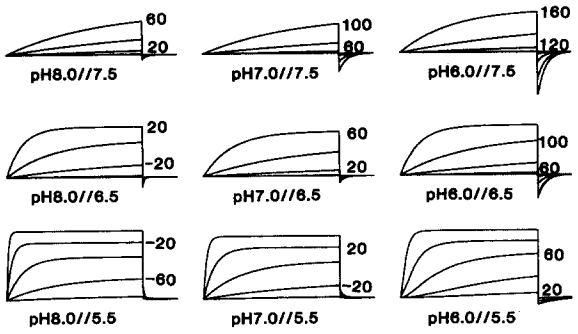

FIGURE 12. Simulated H^+ currents calculated using the model for the range of pH_o//pH_i illustrated in Fig. 3.

formulae from the Appendix and the ΔpH-dependent voltage shift displays saturation at high pH_o.

Proton wells. Suppose that the wings do not carry charge, $m = 0$, and the whole voltage dependence originates from proton adsorption in wells inside the membrane potential field. In that case $\delta_{in} + \delta_{out} = 1.42$, or, if the inner and outer wells are similar, $\delta_{in} = \delta_{out} = 0.71$. The calculated dependence of g_H-V on pH is shown in Fig. 11 *A*, which resembles the data in Fig. 6, as well as the results for the charged-wings model. Both versions of the model predict similar ΔpH dependence of the steady state conductance. The only difference is that at saturation ($pH_o > 9$) the slope of the g_H-V curve becomes two times shallower in the proton well version.

Kinetics. Having found these basic parameters we addressed the kinetic processes of channel opening and closing. We found it impossible to reach a reasonable agreement between theory and experiment if the wings were supposed to be identical. We tried to make the difference between wings as small as possible. Therefore, we kept all the equilibrium constants the same, and the only differences we introduced were different rates of protonation and deprotonation of the two wings at the inner side of membrane. All the other parameters of the wings are the same. Because the agreement between theory and experiment happened to be better in the proton well version of the butterfly model, this was used to generate the simulations shown here. The calculated time-courses of H^+ currents at different potentials, pH_o, and pH_i in Fig. 12 reproduce all of the major features of the real data in Fig. 3. The calculated I'_H-V relationships in Fig. 11 *B* are similar at any given ΔpH, as were the

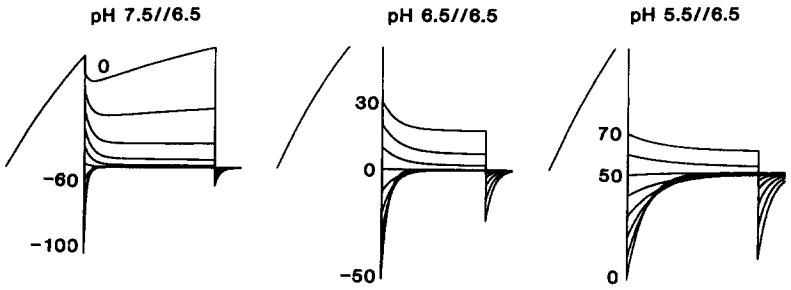

FIGURE 13. Simulated H^+ tail currents calculated for conditions like those in Fig. 9, *A–C*.

Published June 1, 1995

experimental relationships in Fig. 8 *B*. The calculated I'_H at pH_i 7.5 diverges increasingly from calculated values for large depolarizations at the same ΔpH but lower absolute pH, with the divergence becoming marked at pH_o 9 (*left-most dashed curve*). The smaller shift between pH_o 8 and 9 is also evident in this figure (*two left-most dashed curves*), which corresponds with the data in Fig. 8 *A*, and reflects the approach of pH_o to pK_{out}. Finally, tail currents generated with the model (Fig. 13) reproduce the main features of the tail current data in Fig. 9. All of these curves were calculated with the same set of parameters (Fig. 10). We believe that the model is able to account for the fundamental properties of both steady state and kinetic observations.

DISCUSSION

We have characterized the pH_o and pH_i dependence of H^+ current gating over a wide ΔpH range. By using high buffer concentrations and extracellular EGTA, we observed behavior more consistent than in most previous studies. The close correlation of measured V_{rev} and E_H indicates a very high H^+ selectivity ($P_{TMA}/P_H < 10^{-7}$). In previous studies, V_{rev} generally deviated from E_H in being more positive (DeCoursey, 1991; Demaurex et al., 1993; DeCoursey and Cherny, 1993; Bernheim et al., 1993; Kapus, Romanek, and Grinstein, 1994), consistent with the interpretation that H^+ efflux during the prepulse increased pH_i. This explanation cannot be applied to the present data, because the small deviation of V_{rev} from E_H appeared to be directly proportional to ΔpH (Fig. 2). Conceivably TMA^+ might be weakly permeant, but more likely, the local pH near H^+ channels deviates slightly from the bulk pH. Even so, the largest combined deviation of pH_o and pH_i was 0.3 U at pH 8.0//5.5, indicating that over a wide range the local pH was well controlled and similar to nominal bulk values in both bath and pipette solutions. Thus, measurement of V_{rev} is a good indicator of the actual pH gradient across the membrane.

The G_H Amplitude is Practically Independent of H^+ Concentration

Remarkably, the amplitude of the H^+ conductance was nearly independent of pH_i over the range 5.5–7.5. The data are compatible with a small effect of pH_i on the amplitude of H^+ currents. For large depolarizations both I_H and G_H were up to ~50% smaller at pH_i 7.5 than at pH_i 6.5 or 5.5 (Figs. 4 and 6). When one considers that the permeant ion concentration was varied 100-fold bilaterally, this seems a small effect indeed. In previous studies g_H or $g_{H,max}$ was increased by lowering pH_i, either by a small amount (Byerly et al., 1984; Mahaut-Smith, 1989*a*; Demaurex et al., 1993) as in the present results, or substantially (Kapus et al., 1993). However, when direct comparison was made at fixed ΔpH, by means of simultaneous bilateral variation of pH, I_H and g_H were practically constant over a wide range of pH encompassing physiological values. In conclusion, lowering pH_i in an intact cell will tend to activate the g_H at any given membrane potential, however, the mechanism primarily responsible is a shift in the voltage dependence of the g_H-V relation.

Is the Single-Channel Conductance pH Independent?

The near constancy of the g_H between pH_i 5.5–7.5 at constant ΔpH has intriguing implications. Either the single-channel H^+ conductance is constant over this pH range, or the number of conducting channels must increase by the same factor that the unitary conductance decreases, i.e., by an order-of-magnitude/U pH if the GHK equation is used to predict the unitary current. The latter possibility might apply if H_i^+ blocked or otherwise reduced the effective number of conducting H^+ channels: 99% of the H^+ channels that are open at pH_i 7.5 would have to be blocked or closed at pH_i 5.5. Such a mechanism appears to require that H_i^+ both activates and inhibits H^+ channel opening. Given the approximate ΔpH dependence of most of the behavioral features of H^+ currents, and the similarity of the limiting g_H over a wide range of pH_o and pH_i, a simpler hypothesis is that the number of H^+ channels available to open and the single channel H^+ conductance are essentially constant over the entire pH range studied. This conclusion suggests that the rate-limiting step in H^+ conduction is pH-independent.

The pH Independence of the g_H Is Not Due to Diffusion Limitation

Possible rate-limiting steps in H^+ permeation include those considered for ordinary ion channels by Andersen (1983): diffusion through the aqueous phases to and from the channel, channel entry and exit, and channel permeation. Special properties of protons present additional possibilities: buffer deprotonation/protonation reactions, hydrolysis (cf Kasianowicz, Benz, and McLaughlin, 1987), or breaking hydrogen bonds between neutral water molecules (Nagle, 1987). Diffusion of H^+ (or H_3O^+) in bulk solution would occur far too slowly (due to $[H_3O^+]$ being four to six orders of magnitude lower than [BH]) to support the magnitude of I_H observed (DeCoursey, 1991; DeCoursey and Cherny, 1994*b*). Therefore, buffer shuttles protons to the vicinity of the membrane (cf Gutknecht and Tosteson, 1973). If diffusion of buffer through the tip of the pipette were rate-limiting (cf Mathias, Cohen, and Oliva, 1990), manifestations would have a relatively slow time course (seconds), I_H would not simply scale down at all potentials, and furthermore the limiting current would depend on tip geometry and not on cell size.

If hydrolysis, the diffusion of buffer to the vicinity of the membrane, or diffusion-limited buffer deprotonation/reprotonation reactions (Eigen, 1964) were rate limiting, the effect would be manifest as saturation of the H^+ current at a voltage-independent limit during large pulses (cf Andersen, 1983). This is so because all of these mechanisms place the limitation to the unitary H^+ conductance mainly outside the membrane potential field. We observed precisely this phenomenon in alveolar epithelial cells perfused with 5 mM pipette buffer (DeCoursey, 1991). However, in the present experiments with 20-fold higher buffer concentrations, we did not observe current limiting up to as large voltages as the membrane tolerated; the I_0-V relation was superlinear at symmetrical pH up to +140 mV (Fig. 5). Therefore, the I_H amplitude must be determined at the level of the channel and must involve a voltage-dependent process, either permeation itself or a voltage-dependent step in channel entry or exit.

How Does H^+ Permeation Work?

It appears likely that H^+ permeates all channels, from gramicidin to the F_0 component of H^+-ATPases, by a two-step (hop-turn) mechanism in which protons hop across a hydrogen-bonded chain, after which the molecules or groups forming the chain must reorient before another proton can enter the chain (Nagle and Morowitz, 1978; Nagle and Tristram-Nagle, 1983). In ice, the hopping of a proton across a hydrogen-bonded chain is very rapid and reorientation is rate determining (Nagle and Tristram-Nagle, 1983). By analogy with H^+ conductance in ice, where 36% of the full protonic charge translocation occurs during the turning step and the rest during the hopping step (Scheiner and Nagle, 1983), both steps are likely voltage dependent. Because entry of the turning defect into the hydrogen-bonded chain is initiated by the breaking of hydrogen bonds between neutral water molecules, it is essentially pH independent (Nagle, 1987). A logical conclusion is that the rate-limiting step in H^+ permeation may be the entry of the turning defect into the putative hydrogen-bonded chain.

The kinetic competence of hydrogen-bonded chains to conduct protons much faster than the turnover rate of H^+-ATPases, ~1,200 H^+/s (Läuger, 1991), or a 10 fS H^+ channel conductance (10^4 H^+/s at 150 mV), has been demonstrated by theory, using assumptions favorable to rapid permeation (Nagle and Morowitz, 1978; Schulten and Schulten, 1985), and by experiment. The H^+ conductance of the water-filled pore of gramicidin is prodigious, with single-channel H^+ currents saturating at 140 pA at >3 M HCl (Akeson and Deamer, 1991). The apparently much lower conductance of voltage-activated H^+ channels seems incompatible with a water-filled pore, and suggests instead a hydrogen-bonded chain mechanism involving protein side groups, allowing tight control by a gating process and a conductance which saturates at five to six orders of magnitude smaller [H^+].

How Large Can H^+ Channel Currents Be?

The unitary H^+ current through gramicidin channels appears to be diffusion-limited (Decker and Levitt, 1988) and is directly proportional to [H^+] over a wide range from pH 0 to pH 4 (references in DeCoursey and Cherny, 1994*b*), to pH 7.5 (Krishnamoorthy, 1986) or even pH 8.5 (Gutknecht, 1987). Extrapolation of unitary H^+ currents measured at much lower pH in a variety of other H^+ permeable channels, on the assumption that the conductance is proportional to [H^+], gives <1 fA at pH 6 and <0.1 fA at pH 7 for a 100 mV driving force (DeCoursey and Cherny, 1994*b*). The convergence permeability of an H^+ channel calculated for conditions used here according to a model which includes a small enhancement by buffer (by a factor of 1.26–1.42) predicts the maximum single-channel H^+ current to be limited by diffusion to 21 fA at pH 5.5, 2.3 fA at pH 6.5, and 0.23 fA at pH 7.5 (Nunogaki and Kasai, 1988).

Based on H^+ current fluctuation measurements, the unitary H^+ channel conductance is <50 fS at pH_i 5.9 (Byerly and Suen, 1989), ~10 fS at pH_i 6.0 (DeCoursey and Cherny, 1993), and ≤90 fS at pH_i 5.5 (Bernheim et al., 1993). The signal-to-noise ratio was poor in all of these studies, so the estimates must be considered very approximate. These values are comparable with the equivalent H^+ efflux of Na^+-H^+

antiporters at their maximum turnover rate, 0.5 fA and 1.7 fA, at pH_i 6.0 in normal and transformed human fibroblasts, respectively (Siczkowski, Davies, and Ng, 1994). Given the apparent pH-independence of the g_H and the estimate of 10 fS for the unitary conductance of H^+ channels at pH 6, the unitary H^+ current at pH_i 7.5 is evidently significantly larger than the diffusion-limited predictions above (0.1–0.23 fA). The F_0 component of H^+-ATPase also is a proton channel with a unitary conductance independent of pH over the range pH 5.6–8.0 (Althoff, Lill, and Junge, 1989; Wagner, Apley, and Hanke, 1989) and of similar magnitude, 10 fS (Schoenknecht, Junge, Lill, and Engelbrecht, 1986) up to 1 pS (Junge, 1989) depending on assumptions. Several mechanisms which were not included in the above calculations have been discussed in the context of attempts to explain how such large proton fluxes can be sustained by diffusion at physiological pH: local concentration of H^+ by charges on the membrane or channel, a large vestibule, buffering by membrane lipids, hydrolysis, or rapid surface conduction of protons (Haines, 1983; Nachliel and Gutman, 1984; Schulten and Schulten, 1985; Nagle and Dilley, 1986; Prats, Tocanne, and Teissie, 1987; Kasianowicz et al., 1987; Althoff et al., 1989; Junge, 1989; Wagner et al., 1989). Electrodiffusion may further enhance the supply of protons (but not of neutral BH) to the channel, increasing the effective pore radius by one Debye length (Peskoff and Bers, 1988).

THE VOLTAGE DEPENDENCE OF H^+ CHANNEL GATING IS SET BY ΔpH

pH_o and pH_i Shift H^+ Current Activation According to ΔpH

A defining characteristic of voltage-activated H^+ channels is that their voltage-activation curve is shifted to more negative potentials by increased pH_o or decreased pH_i. The magnitudes of these effects varied in previous studies, and no quantitative relationship had been described. We show here that over the range of pH_i 5.5–7.5 and pH_o 6.0–8.0, I_H-V relationships shifted by ~40 mV/U pH, and were essentially identical at a given ΔpH. In other words, the shift was directly proportional to ΔpH, and pH_o and pH_i were equally effective in shifting the voltage dependence of H^+ channel gating. The effect of pH_o exhibited saturation, such that the shifts of I_H-V, g_H-V, or I'_H-V between pH_o 8 and 9 were less than at lower pH. This result is consistent with an externally accessible protonation site with a pK ~8.5 (cf Fig. 11 *B*). The g_H-V relation in snail neurons was shifted −46 mV between pH_o 6.4 and 7.4, but no further shift was seen at pH_o 8.4 (Byerly et al., 1984) consistent with a similar mechanism with a lower pK than in alveolar epithelial H^+ channels. Qualitatively similar saturation of the g_H-V shift at high pH_o occurs in *Ambystoma* (Barish and Baud, 1984) and murine macrophages (Kapus et al., 1993).

Another ion channel whose voltage-dependent gating depends on permeant ion concentration is the inward rectifier K^+ channel (Hagiwara and Takahashi, 1974). Both activation and deactivation kinetics of some inward rectifier channels shift precisely with V-V_K when $[K^+]_o$ is varied (Saigusa and Matsuda, 1988; Silver and DeCoursey, 1990); in other cells the shifts are unequal (Pennefather, Oliva, and Mulrine, 1992). For H^+ channels, V_{rev} measured under identical conditions in the same cells varied by 52 mV/U ΔpH, a significantly larger shift than that of steady

state gating or kinetic parameters. Thus, H^+ channel gating cannot be defined strictly as (V-E_H) dependent, but as ΔpH dependent. The magnitude of the shift of various parameters with ΔpH varied. The voltage dependence of I_H, g_H, the rate of activation (I'_H), and the slow component of deactivation (τ_{slow}) all shifted ~40 mV/ΔpH. In contrast, τ_{fast} was much less sensitive, shifting only ~20 mV/U ΔpH or less. I'_H appeared to increase with ΔpH in addition to shifting along the voltage axis. To a first approximation, however, the behavior of the g_H was the same at any given ΔpH. Given these general similarities, it is not surprising that our model shares some features of models proposed to account for gating of inward rectifier K^+ channels (Ciani, Krasne, Miyazaki, and Hagiwara, 1978; Pennefather et al., 1992; Pennefather and DeCoursey, 1994). The equivalence of voltage and pH suggests a parallel with the concept of ion wells or access channels as proposed for the H^+-ATPase (Mitchell and Moyle, 1974; Läuger, 1991) and the Na^+/K^+-ATPase (Gadsby et al., 1993; Hilgemann, 1994; De Weer et al., 1994). In the latter case, the access channel for Na^+ senses ~70% of the membrane potential (Gadsby et al., 1993). The proton well version of our model incorporates voltage-dependent proton binding in external and internal proton wells, each sensing 71% of the membrane potential.

Practical Consequences: Predicting g_H Activation in Intact Cells

By extrapolating the present results to behavior in intact cells, the following relationship was distilled from the data in order to predict the "threshold" potential at which activation is first detectable:

$$V_{threshold}(mV) = V_0 - 40\Delta pH \quad (6)$$

where ΔpH is defined as used in this paper: $\Delta pH = pH_o - pH_i$, and V_0 is $V_{threshold}$ at symmetrical pH (i.e., when ΔpH = 0). In many cells V_0 was +20 mV, but sometimes it was +40 mV (we normally used 20-mV voltage increments). There was cell-to-cell variability in V_0, but the shift in any given cell of −40 mV/U pH_o was quite consistent. Recognizing that no sharply distinguishable threshold potential actually exists, $V_{threshold}$ provides a useful if arbitrary guide. Considering the absence of depolarization-activated inward currents (DeCoursey et al., 1988), the resting potential of intact alveolar epithelial cells probably does not exceed $V_{threshold}$ by much, and the voltage dependence of the g_H is steep enough that within a few mV enough H^+ channels will be activated to increase pH_i or to repolarize the membrane potential. The relationship in Eq. 6 applies only to the conditions of our study; the pH sensitivity of the g_H may vary in different cell types or may be modulated by cytokines. For example, arachidonic acid enhances the g_H in phagocytes (Henderson and Chappell, 1992) by shifting the voltage-activation curve to more negative potentials (DeCoursey and Cherny, 1993; Kapus et al., 1994).

An intriguing prediction of Eq. 6 is that at a large negative ΔpH steady state inward H^+ currents should occur. In fact, $V_{threshold}$ was close to V_{rev} at pH 6.0//7.5 (ΔpH = −1.5), where activation of the g_H could best be detected indirectly, by observing the tail current after depolarizing pulses. In an intact cell inward I_H would depolarize the membrane and further activate the g_H like the regenerative activation of Na^+ channels during action potentials in excitable tissues. It is obviously unlikely that an intact cell could achieve these conditions, so it remains true that over the

physiologically relevant range of pH and membrane potentials H^+ channels only conduct outward steady state currents.

PROPERTIES OF H^+ CHANNELS

Instantaneous Rectification

The I_0-V relationship rectified outwardly at symmetrical pH, with a slope conductance about twice as large at positive than at negative potentials (rectification ratio = 2). Rectification was more pronounced at higher ΔpH, in the direction expected from the GHK current equation, e.g., at ΔpH = 1.5 the rectification ratio increased to ≥3. However, the GHK equation predicts that changing ΔpH from 0 to 1.5 ought to increase the rectification ratio from 1.0 to 31.6, and therefore cannot be used to predict rectification of H^+ currents. Previously, the I_0-V relation was described as approximately linear or slightly outwardly rectifying. Because the rectification is fairly gradual, over a narrow voltage range the I_0-V relation appears to be approximately linear. For this reason, correcting the G_H-V relation for rectification had only a subtle effect. That H^+ moves outwardly more readily than inwardly suggests that the H^+ permeation pathway is asymmetrical.

H^+ Channel Gating

The data provide a number of empirical constraints on the mechanism of H^+ channel gating. The sigmoid time course of mammalian H^+ current activation suggests that the channels traverse at least two closed states before opening (DeCoursey and Cherny, 1994*b*). We could not fit the activation time course with a Hodgkin-Huxley parameter raised to a fixed exponent, which argues against the simplest case of independent conformational changes in two or more identical channel protomers to form a conducting pore. The next most parsimonious scheme is two sequential kinetically distinct transitions:

$$\underset{\text{slow}}{C_1} \leftrightarrow C_2 \underset{\beta}{\overset{\alpha}{\rightleftharpoons}} \underset{\text{fast}}{O}.$$

H^+ current deactivation was noted to be faster at more negative potentials in previous studies (Barish and Baud, 1984; DeCoursey, 1991; Kapus et al., 1994), but its voltage and pH dependence was not investigated systematically. Tail currents after depolarizing prepulses decayed exponentially at potentials well negative to V_{rev}, but a second, slower component of decay became evident at potentials near threshold, which coincidentally is the most physiologically relevant range. Two components of I_H decay indicate the existence of at least three states. Because τ_{fast} and τ_{slow} differed at some potentials by an order of magnitude or more, the two steps evidently have widely different kinetics, again inconsistent with an n^2 model in which the τ's would differ only by a factor of two (Bernasconi, 1976; Zagotta, Hoshi, Dittman, and Aldrich, 1994). At large negative potentials τ_{tail} reflects mainly β, because α is likely small when $P_{open} \simeq 0$. Single exponential decay with $\tau \approx 1/\beta$ would be expected if $C_1 \leftrightarrow C_2$ transitions are relatively slow. The voltage dependence of the τ_{tail} in this

region was weak, 40–60 mV/e-fold change in potential, and was approximately exponentially voltage dependent. In contrast, τ_{slow} was steeply voltage dependent, changing e-fold in 8–15 mV. These results suggest that the process reflected in τ_{slow} includes most of the charge movement of gating.

An intriguing result is that τ_{fast} was the least sensitive of any parameter studied to changes in ΔpH, shifting at most ~20 mV/U ΔpH. In light of its shallow voltage dependence and interference by the slower component, it is possible that this step may be completely independent of pH. τ_{slow} was as sensitive to pH_o as were kinetic and equilibrium indicators of activation. Evidently most of the pH dependence of gating resides in the slower transition as well.

The slower component of tail current decay which becomes pronounced near threshold potentials presumably is attributable to the $C_1 \leftrightarrow C_2$ transition. The faster τ related to the $O \rightarrow C_2$ transition is still present, but because α is now closer to β some channels will reopen and thus a slower component will appear as channels gradually disappear via the $C_2 \rightarrow C_1$ path. Given the above simple three-state scheme, the first step, $C_1 \leftrightarrow C_2$, could not be rapid because then its relaxation would be "filtered" through the slower $O \rightarrow C_2$ transition. At equilibrium the $C_1 \rightarrow C_2$ transition must occur to some extent at more negative potentials than the $C_2 \rightarrow O$ transition. Depolarizing prepulses below threshold reduce the sigmoidicity of activation (DeCoursey and Cherny, 1994*b*), suggesting that a significant fraction of channels can undergo the $C_2 \rightarrow C_1$ transition without opening. As shown in Fig. 9*A*, at some potentials above threshold, the tail current relaxation has a rapidly decaying component and a slower rising component. In other words, the two relaxations proceed in opposite directions, given the same preconditions. This nonmonotonic relaxation argues that the faster component reflects transitions nearer the open state. In summary, any realistic gating model for H^+ channel activation must have at least two distinct steps (≥ three states). A transition remote from the open state appears to be slower and more steeply voltage dependent than a transition nearer the open state. It is not likely that the simplest three-state model can account for all details of gating kinetics.

Gating Model

The proposed model represents a first attempt to demonstrate a mechanism capable of reproducing the main features of H^+ channel gating, specifically the dependence of most parameters on ΔpH, independent of the absolute pH. We kept the assumptions as simple as possible. The voltage dependence of H^+ channel gating is modulated by internal and external protons acting at a site which can be alternately accessible to either solution. The *pK* of the proposed modulatory site was kept the same at the internally and externally accessible configurations ($pK_{in} = pK_{out}$), although the *pK* of the same site could change when the molecule of which it is a part is in a different conformation, like the Schiff base of bacteriorhodopsin (Stoeckenius, Lozier, and Bogomolni, 1979) and as shown by ab initio modeling (Scheiner and Hillenbrand, 1985). The data at this stage do not adequately constrain the model to define the optimum number of wings, or the number of protonation sites per wing. The types of data required for these refinements are being collected. However, the general type of model proposed is feasible. The assumption of alternate access of the

protonation site seemed simpler than proposing distinct protonation sites at either face of the membrane. To account for the large and uniform voltage shifts observed over 2 U pH_o and pH_i, it would be necessary to postulate several independent protonation sites with a range of *pK*'s at both the outer and inner ends of the channel molecule with internal and external sites having equivalent effectiveness in altering the transmembrane potential sensed by the channel's voltage sensor.

Fig. 10 illustrates three physical representations of the mathematical formulation of the gating mechanism in the model. The postulated gross movement of the wings across the entire membrane (Fig. 10 *A*) resembles proposed mechanisms of voltage-dependent gating of a variety of small channel-forming molecules: alamethicin (Woolley and Wallace, 1992), monazomycin (Heyer, Muller, and Finkelstein, 1976), melittin (Kempf, Klausner, Weinstein, Renswoude, Pincus, and Blumenthal, 1982), colicin (Raymond, Slatin, Finkelstein, Liu, and Levinthal, 1986), and synthetic channels (Chung, Lear, and DeGrado, 1992), as well as the larger inward rectifier K^+ channel (Ciani et al., 1978). Another embodiment of the model (Fig. 10 *B*) invokes distinct external and internal regulatory sites, the protonation of either allosterically preventing protonation of the other. A subtle conformational change could also be envisioned (Fig. 10 *C*), e.g., a regulatory protonation site located within bilateral proton wells could by various mechanisms become alternately accessible to the solution on one or the other side of the membrane. Alternating-access mechanisms are considered more plausible for ion pumps than conformational changes requiring large molecular movements (Läuger, 1991). To adequately simulate the data, it was necessary to make the conformational change (between states 2 and 3) more rapid than the protonation/deprotonation steps, consistent with its entailing a small movement. Together with the better fit to the data when the proton well version of the model was assumed (Theoretical section), and the empirical conclusions that most of the voltage dependence and pH dependence of gating reside in a slow step, we conclude that most of the voltage dependence of gating occurs in protonation/deprotonation steps rather than in the conformational change.

That the rapid component of deactivation (τ_{fast}) shifted much less with pH_o than the other parameters is intriguing in light of our interpretation that τ_{fast} represents the first (or an early) closing transition. If the regulatory protonation site were in the conduction pathway (analogous to the pore of a normal ion channel) it might be unable to sense pH_o and pH_i when the channel is open, because the open channel H^+ conductance is essentially pH independent. All other kinetic transitions occur between closed states, i.e., in the absence of H^+ efflux, and these parameters shifted uniformly $\sim$40 mV/U ΔpH. Therefore, it seems possible that the regulatory protonation site(s) may be in the conduction pathway itself.

APPENDIX

The Model and Constitutive Equations

In the section Theoretical we introduced the butterfly model of a proton channel with four states for each wing defined in Fig. 10. We consider here an arbitrary number of wings, j. Because of electrogenic properties of transitions between different states, the rates of these transitions can be presented (Markin and Chizmadzhev, 1974; Markin,

Pastushenko, and Chizmadzhev, 1987) in the following way:

$$r_{12} = k_{12} \exp\left(\frac{ne_0\delta_{out}V}{2k_BT}\right), \tag{A.1}$$

$$r_{21} = k_{21}[H^+]^n_{out} \exp\left(-\frac{ne_0\delta_{out}V}{2k_BT}\right), \tag{A.2}$$

$$r_{23} = k_{23} \exp\left(\frac{me_0V}{2k_BT}\right), \tag{A.3}$$

$$r_{32} = k_{32} \exp\left(-\frac{me_0V}{2k_BT}\right), \tag{A.4}$$

$$r_{34} = k_{34}[H^+]^n_{in} \exp\left(\frac{ne_0\delta_{in}V}{2k_BT}\right), \tag{A.5}$$

$$r_{43} = k_{43} \exp\left(-\frac{ne_0\delta_{in}V}{2k_bT}\right). \tag{A.6}$$

The variation of the probabilities of different states P_1, P_2, P_3, and P_4 (for each wing considered alone) are determined by the following equations:

$$\frac{dP_1}{dt} = -r_{12}P_1 + r_{21}P_2, \tag{A.7}$$

$$\frac{dP_2}{dt} = r_{12}P_1 - (r_{21} + r_{23})P_2 + r_{32}P_3, \tag{A.8}$$

$$\frac{dP_3}{dt} = r_{23}P_2 - \{r_{32} + r_{34}\}P_3 + r_{43}P_4, \tag{A.9}$$

$$P_1 + P_2 + P_3 + P_4 = 1. \tag{A.10}$$

Because each of j protomers can be in four states, the total number of states is 4^j. But the channel is open only if all j wings are in the fourth state, i.e., they are down and protonated. To permit assigning different H^+ affinity or kinetic properties for the different wings, we distinguish the corresponding probabilities: $P_4^{(1)}$, $P_4^{(2)}$, . . . , $P_4^{(j)}$. The probability of the open state of the channel is the product of corresponding probabilities: $P_{open} = P_4^{(1)} P_4^{(2)} \ldots P_4^{(j)}$. If the limiting conductance is $g_{H,max}$, then the conductance at a given voltage is

$$g_H(V) = g_{H,max}P_4^{(1)}P_4^{(2)} \ldots P_4^{(j)}. \tag{A.11}$$

Let us introduce also equilibrium proton dissociation constants

$$K_{out} = \frac{k_{12}}{k_{21}} \quad \text{and} \quad K_{in} = \frac{k_{43}}{k_{34}}, \tag{A.12}$$

and an equilibrium wing conformation constant

$$K_w = \frac{k_{32}}{k_{23}}. \tag{A.13}$$

The latter constant gives the ratio between "up" and "down" (or out and in) conformations of deprotonated wings in the absence of electrical field (i.e., at 0 mV). It may be convenient to use the pK of acid groups inside and outside membrane:

$$pK_{in} = -\frac{1}{n}\log K_{in} \quad \text{and} \quad pK_{out} = -\frac{1}{n}\log K_{out}. \tag{A.14}$$

We shall use a pH difference in the form

$$\Delta pH = pH_o - pH_i, \tag{A.15}$$

and the Nernst potential for protons

$$E_H = -\frac{2.3k_BT}{e_0}\Delta pH. \tag{A.16}$$

Steady State Regime

For the beginning let us consider our system in a steady state. Solving the set of Eqs. A.7–A.10 one obtains:

$$P_1 = P_4K_w \exp\left[2.3n(pH_i - pH_o - pK_{in} + pK_{out}) - \frac{me_0V}{k_bT} - \frac{ne_0(\delta_{in} + \delta_{out})V}{k_BT}\right], \tag{A.17}$$

$$P_2 = P_4K_w \exp\left[2.3n(pH_i - pK_{in}) - \frac{me_0V}{k_BT} - \frac{ne_0\delta_{in}V}{k_BT}\right], \tag{A.18}$$

$$P_3 = P_4 \exp\left[2.3n(pH_i - pK_{in}) - \frac{ne_0\delta_{in}V}{k_BT}\right], \tag{A.19}$$

$$P_4 = \left\{\begin{array}{l} 1 + \exp\left[2.3n(pH_i - pK_{in}) - \dfrac{ne_0\delta_{in}V}{k_BT}\right] \\ \quad * \left\{1 + K_w \exp\left(-\dfrac{me_0V}{k_BT}\right)\left[1 + \exp\left[2.3n(pK_{out} - pH_o) - \dfrac{ne_0\delta_{out}V}{k_BT}\right]\right]\right\} \end{array}\right\}^{-1}. \tag{A.20}$$

Let us suppose for the sake of simplicity that equilibrium constants of all wings are the same. Then substituting these formulas into Eq. A.11 one can find conductance of the system:

$$\frac{g_H}{g_{H,max}} = \left\{\begin{array}{l} 1 + \exp\left[2.3n(pH_i - pK_{in}) - \dfrac{ne_0\delta_{in}V}{k_BT}\right] \\ \quad * \left\{1 + K_w \exp\left(-\dfrac{qV}{k_BT}\right)\left[1 + \exp\left[2.3n(pK_{out} - pH_o) - \dfrac{ne_0\delta_{out}V}{k_BT}\right]\right]\right\} \end{array}\right\}^{-j}. \tag{A.21}$$

This equation gives a steady state conductance as the function of membrane voltage and proton concentrations at both sides of membrane. These rather cumbersome expressions drastically simplify in a practically important particular case. Suppose that the pK's of acidic groups are rather high so that proton concentrations at both sides exceed the dissociation constant:

$$pK_{in} > pH_i \quad \text{and} \quad pK_{out} > pH_o. \tag{A.22}$$

In that case, acidic groups are almost saturated and the expression for probability P_4 simplifies to

$$P_4 = \left\{1 + \exp\left[\ln K_w + 2.3n(\Delta pK - \Delta pH) - \frac{me_0 + ne_0(\delta_{in} + \delta_{out})}{k_B T} V\right]\right\}^{-1}. \tag{A.23}$$

This is a Boltzmann function of the type $1/(1 + e^{a-bV})$ with parameters

$$a = \ln K_w + 2.3n(\Delta pK - \Delta pH), \tag{A.24}$$

and

$$b = \frac{me_0 + ne_0(\delta_{in} + \delta_{out})}{k_B T}. \tag{A.25}$$

Open probability simplifies to

$$\frac{g_H}{g_{H,max}} = P_{open} = \left\{1 + \exp\left[\ln K_w + 2.3n(\Delta pK - \Delta pH) - \frac{me_0 + ne_0(\delta_{in} + \delta_{out})}{k_B T} V\right]\right\}^{-j}. \tag{A.26}$$

This expression is not an exact Boltzmannian, but it is very close to this function, though with different parameters. If the butterfly has only one wing, then $P_{open} = P_4$. With increasing numbers of wings, the open probability shifts to the right and slope steepens. If open probability is presented in the form

$$\frac{g_H}{g_{H,max}} = \frac{1}{1 + \exp\left(\frac{V_{1/2} - V}{V_{slope}}\right)} \tag{A.27}$$

with the half-activation potential $V_{1/2}$ and slope factor V_{slope}, then one can establish the relationship between these factors and a and b:

$$V_{1/2} = \frac{a - \ln(2^{1/j} - 1)}{b} \quad \text{and} \quad V_{slope} = \frac{1}{2j(1 - 2^{-1/j})b}. \tag{A.28}$$

For $j = 1$ these two factors, as expected, are correspondingly a/b and $1/b$.
For $j = 2$ they are $(a + 0.881)/b$ and $1/(1.17b)$.
For $j = 3$ they are $(a + 1.347)/b$ and $1/(1.23b)$.
For $j = 4$ they are $(a + 1.665)/b$ and $1/(1.27b)$.
For $j = 5$ they are $(a + 1.906)/b$ and $1/(1.29b)$ and so on.

Therefore, if the pK's are high enough, the conductance is a Boltzmann function of membrane potential and of ΔpH and it does not depend on the magnitude of pH at

each side. With variation of ΔpH the half activation potential shifts as

$$\Delta V_{1/2} = \frac{2.3nk_BT}{e_0[m + n(\delta_{in} + \delta_{out})]}\Delta pH. \quad (A.29)$$

Interestingly enough, this shift does not depend on the number of wings. But the slope of voltage dependence of conductance does depend on the number of wings:

$$V_{slope} = \frac{k_BT}{2j(1 - 2^{-1/j})e_0[m + n(\delta_{in} + \delta_{out})]}. \quad (A.30)$$

This gives the opportunity to establish relationship between $\Delta V_{1/2}$ and V_{slope}:

$$\Delta V_{1/2} = -4.6j(1 - 2^{-1/j})nV_{slope}\Delta pH, \quad (A.31)$$

Because $\Delta V_{1/2}/\Delta pH$ and V_{slope} can be found in experiment, Eq. A.31 permits finding the number of protons per one wing:

$$n = -\frac{1}{4.6j(1 - 2^{-1/j})V_{slope}}\left(\frac{\Delta V_{1/2}}{\Delta pH}\right). \quad (A.32)$$

The numerical coefficient $4.6j(1 - 2^{-1/j})$ in the denominator of this equation has an interesting structure: it does not change very much with the number of wings. At j = 1 it is equal to 2.3, at j = 2 to 2.70, at j = 3 to 2.83, at j = 4 to 2.93 and at j = 5 to 2.98. Even if j goes to infinity the limiting value of this coefficient is not very large: it is 3.188. Therefore the number of protons adsorbed at one wing can be estimated from experimental data reliably enough even if the number of wings is unknown.

Relatively simple equations derived above were obtained under supposition that pH inside and outside the cell does not exceed the *pK* of binding sites for protons. In this case both charge of the wing and charge of the protons adsorbed in the wells enter the equations in the same single combination $e_0[m + n(\delta_{in} + \delta_{out})]$. Therefore in this domain both versions of the butterfly model predict the same potential dependence of the steady state conductance. But in a more general case the steady state conductance can be obtained from general Eq. A21. The difference between proton wells and charged wing versions on the butterfly model manifests itself at saturation: the proton wells version saturates at higher pH and the slope of conductance changes at saturation. Although the behavior of the $g_H - V$ data at high pH_o more closely resembles that of the charged wings model, the kinetics of H^+ currents was much better predicted by the proton well version.

Therefore, steady state measurements permit finding the number of protons per wing, the depth of proton wells, and the charge of the wings. But these measurements are rather insensitive to the number of wings in the channel complex and of course they do not give the opportunity to find the rate constants. These parameters can be found in the kinetic measurements.

Kinetics

Some general conclusions can be derived from the analysis of the general kinetic equations, but the most detailed information was obtained as a result of numerical

solution of these equations. The results are presented in Figs. 11 *B*, 12, and 13. It was found impossible to simulate with one wing only.

We appreciate the technical assistance of Donald R. Anderson.

This work was supported by a Grant-in-Aid from the American Heart Association to T. E. DeCoursey, and by salary support for V. S. Markin from NIH grant DC00241 to A. J. Hudspeth.

Original version received 3 October, 1994 and accepted version received 9 February 1995.

REFERENCES

Akeson, M., and D. W. Deamer. 1991. Proton conductance by the gramicidin water wire: model for proton conductance in the F_0F_1 ATPases? *Biophysical Journal.* 60:101–109.

Althoff, G., H. Lill, and W. Junge. 1989. Proton channel of the chloroplast ATP synthase, CF_0: its time-averaged single-channel conductance as a function of pH, temperature, isotopic and ionic medium composition. *Journal of Membrane Biology.* 108:263–271.

Andersen, O. S. 1983. Ion movement through gramicidin A channels: studies on the diffusion-controlled association step. *Biophysical Journal.* 41:147–165.

Barish, M. E., and C. Baud. 1984. A voltage-gated hydrogen ion current in the oocyte membrane of the axolotl, *Ambystoma. Journal of Physiology.* 352:243–263.

Bernasconi, C. F. 1976. Relaxation Kinetics. Academic Press, New York. 288 pp.

Bernheim, L., R. M. Krause, A. Baroffio, M. Hamann, A. Kaelin, and C.-R. Bader. 1993. A voltage-dependent proton current in cultured human skeletal muscle myotubes. *Journal of Physiology.* 470:313–333.

Byerly, L., R. Meech, and W. Moody. 1984. Rapidly activating hydrogen ion currents in perfused neurones of the snail, *Lymnaea stagnalis. Journal of Physiology.* 351:199–216.

Byerly, L., and W. J. Moody. 1986. Membrane currents of internally perfused neurones of the snail, *Lymnaea stagnalis,* at low intracellular pH. *Journal of Physiology.* 376:477–491.

Byerly, L., and Y. Suen. 1989. Characterization of proton currents in neurones of the snail, *Lymnaea stagnalis. Journal of Physiology.* 413:75–89.

Chung, L. A., J. D. Lear, and W. F. DeGrado. 1992. Fluorescence studies of the secondary structure and orientation of a model ion channel peptide in phospholipid vesicles. *Biochemistry.* 31:6608–6616.

Ciani, S., S. Krasne, S. Miyazaki, and S. Hagiwara. 1978. A model for anomalous rectification: electrochemical-potential-dependent gating of membrane channels. *Journal of Membrane Biology.* 44:103–134.

Decker, E. R., and D. G. Levitt. 1988. Use of weak acids to determine the bulk diffusion limitation of H^+ ion conductance through the gramicidin channel. *Biophysical Journal.* 53:25–32.

DeCoursey, T. E. 1990. State-dependent inactivation of K^+ currents in rat type II alveolar epithelial cells. *Journal of General Physiology.* 95:617–646.

DeCoursey, T. E. 1991. Hydrogen ion currents in rat alveolar epithelial cells. *Biophysical Journal.* 60:1243–1253.

DeCoursey, T. E., and V. V. Cherny. 1993. Potential, pH, and arachidonate gate hydrogen ion currents in human neutrophils. *Biophysical Journal.* 65:1590–1598.

DeCoursey, T. E., and V. V. Cherny. 1994*a*. Na^+-H^+ antiport detected through hydrogen ion currents in rat alveolar epithelial cells and human neutrophils. *Journal of General Physiology.* 103:755–785.

DeCoursey, T. E., and V. V. Cherny. 1994*b*. Voltage-activated hydrogen ion currents. *Journal of Membrane Biology.* 141:203–223.

DeCoursey, T. E., E. R. Jacobs, and M. R. Silver. 1988. Potassium channels in rat type II alveolar epithelial cells. *Journal of Physiology.* 395:487–505.

Demaurex, N., S. Grinstein, M. Jaconi, W. Schlegel, D. P. Lew, and K.-H. Krause. 1993. Proton currents in human granulocytes: regulation by membrane potential and intracellular pH. *Journal of Physiology.* 466:329–344.

De Weer, P., R. F. Rakowski, and D. C. Gadsby. 1994. Voltage sensitivity of the Na^+/K^+ pump: structural implications. *In* The Sodium Pump: Structure Mechanism, Hormonal Control and its Role in Disease. E. Bamberg and W. Schoner, editors. Dietrich Steinkopff Verlag, Darmstadt, Germany. 472–481.

Eigen, M. 1964. Proton transfer, acid-base catalysis, and enzymatic hydrolysis. Elementary processes. *Angewandte Chemie, International Edition.* 3:1–19.

Gadsby, D. C., R. F. Rakowski, and P. De Weer. 1993. Extracellular access to the Na,K pump: pathway similar to ion channel. *Science.* 260:100–103.

Gutknecht, J. 1987. Proton conductance through phospholipid bilayers: water wires or weak acids? *Journal of Bioenergetics and Biomembranes.* 19:427–442.

Gutknecht, J., and D. C. Tosteson. 1973. Diffusion of weak acids across lipid bilayer membranes: effects of chemical reactions in the unstirred layers. *Science.* 182:1258–1261.

Hagiwara, S., and K. Takahashi. 1974. The anomalous rectification and cation selectivity of the membrane of a starfish egg cell. *Journal of Membrane Biology.* 18:61–80.

Haines, T. H. 1983. Anionic lipid headgroups as a proton-conducting pathway along the surface of membranes: a hypothesis. *Proceedings of the National Academy of Sciences, USA.* 80:160–164.

Hamill, O. P., A. Marty, E. Neher, B. Sakmann, and F. J. Sigworth. 1981. Improved patch-clamp techniques for high-resolution current recording from cells and cell-free membrane patches. *Pflügers Archiv.* 391:85–100.

Henderson, L. M., and J. B. Chappell. 1992. The NADPH-oxidase-associated H^+ channel is opened by arachidonate. *Biochemical Journal.* 283:171–175.

Heyer, E. J., R. U. Muller, and A. Finkelstein. 1976. Inactivation of monazomycin-induced voltage-dependent conductance in thin lipid membranes: II. Inactivation produced by monazomycin transport through the membrane. *Journal of General Physiology.* 67:731–748.

Hilgemann, D. W. 1994. Channel-like function of the Na,K pump probed at microsecond resolution in giant membrane patches. *Science.* 263:1429–1432.

Junge, W. 1989. Protons, the thylakoid membrane, and the chloroplast ATP synthase. *Annals of the New York Academy of Sciences.* 574:268–285.

Kapus, A., R. Romanek, and S. Grinstein. 1994. Arachidonic acid stimulates the plasma membrane H^+ conductance of macrophages. *Journal of Biological Chemistry.* 269:4736–4745.

Kapus, A., R. Romanek, A. Y. Qu, O. D. Rotstein, and S. Grinstein. 1993. A pH-sensitive and voltage-dependent proton conductance in the plasma membrane of macrophages. *Journal of General Physiology.* 102:729–760.

Kasianowicz, J., R. Benz, and S. McLaughlin. 1987. How do protons cross the membrane-solution interface? Kinetic studies on bilayer membranes exposed to the protonophore S-13 (5-chloro-3-tert-butyl-2′-chloro-4′nitrosalicylanilide). *Journal of Membrane Biology.* 95:73–89.

Kempf, C., R. D. Klausner, J. N. Weinstein, J. Van Renswoude, M. Pincus, and R. Blumenthal. 1982. Voltage-dependent trans-bilayer orientation of melittin. *Journal of Biological Chemistry.* 257:2469–2476.

Krishnamoorthy, G. 1986. Temperature jump as a new technique to study the kinetics of fast transport of protons across membranes. *Biochemistry.* 25:6666–6671.

Läuger, P. 1986. Barrier models for the description of proton transport across membranes. *Methods in Enzymology.* 127:465–471.

Läuger, P. 1991. Electrogenic Ion Pumps. Sinauer Associates, Sunderland, MA. 313 pp.

Mahaut-Smith, M. 1989*a*. Separation of hydrogen ion currents in intact molluscan neurones. *Journal of Experimental Biology.* 145:439–454.

Mahaut-Smith, M. 1989*b*. The effect of zinc on calcium and hydrogen ion currents in intact snail neurones. *Journal of Experimental Biology.* 145:455–464.

Markin, V. S., and Yu. A. Chizmadzhev. 1974. Induced Ion Transport. Nauka, Moscow. 251 pp.

Markin, V. S., V. F. Pastushenko, and Yu. A. Chizmadzhev. 1987. Theory of Excitable Media. John Wiley and Sons, Inc., New York. 303 pp.

Martell, A. E., and R. M. Smith. 1974. Critical Stability Constants. Volume 1: Amino Acids. Plenum Publishing Corp., New York. 269 pp.

Mathias, R. T., I. S. Cohen, and C. Oliva. 1990. Limitations of the whole cell patch clamp technique in the control of intracellular concentrations. *Biophysical Journal.* 58:759–770.

McGuigan, J. A. S., D. Lüthi, and A. Buri. 1991. Calcium buffer solutions and how to make them: a do it yourself guide. *Canadian Journal of Physiology and Pharmacology.* 69:1733–1749.

Meech, R. W., and R. C. Thomas. 1987. Voltage-dependent intracellular pH in *Helix aspersa* neurones. *Journal of Physiology.* 390:433–452.

Mitchell, P., and J. Moyle. 1974. The mechanism of proton translocation in reversible proton-translocating adenosine triphosphatases. *Biochemical Society Special Publication.* 4:91–111.

Nachliel, E., and M. Gutman. 1984. Kinetic analysis of proton transfer between reactants adsorbed to the same micelle. The effect of proximity on the rate constants. *European Journal of Biochemistry.* 143:83–88.

Nagle, J. F. 1987. Theory of passive proton conductance in lipid bilayers. *Journal of Bioenergetics and Biomembranes.* 19:413–426.

Nagle, J. F., and R. A. Dilley. 1986. Models of localized energy coupling. *Journal of Bioenergetics and Biomembranes.* 18:55–64.

Nagle, J. F., and H. J. Morowitz. 1978. Molecular mechanisms for proton transport in membranes. *Proceedings of the National Academy of Sciences, USA.* 75:298–302.

Nagle, J. F., and S. Tristram-Nagle. 1983. Hydrogen bonded chain mechanisms for proton conduction and proton pumping. *Journal of Membrane Biology.* 74:1–14.

Nunogaki, K., and M. Kasai. 1988. The H^+/OH^- flux localizes around the channel mouth in buffered solutions. *Journal of Theoretical Biology.* 134:403–415.

Pennefather, P., and T. E. DeCoursey. 1994. A scheme to account for the effects of Rb^+ and K^+ on inward rectifier K-channels of bovine artery endothelial cells. *Journal of General Physiology.* 103:549–581.

Pennefather, P., C. Oliva, and N. Mulrine. 1992. Origin of the potassium and voltage dependence of the cardiac inwardly rectifying K-current (I_{K1}). *Biophysical Journal.* 61:448–462.

Peskoff, A., and D. M. Bers. 1988. Electrodiffusion of ions approaching the mouth of a conducting membrane channel. *Biophysical Journal.* 53:863–875.

Prats, M., J. F. Tocanne, and J. Teissie. 1987. Lateral proton conduction at a lipid/water interface. Effect of lipid nature and ionic content of the aqueous phase. *European Journal of Biochemistry.* 162:379–385.

Raymond, L., S. L. Slatin, A. Finkelstein, Q.-R. Liu, and C. Levinthal. 1986. Gating of a voltage-dependent channel (colicin E1) in planar lipid bilayers: translocation of regions outside the channel-forming domain. *Journal of Membrane Biology.* 92:255–268.

Saigusa, A., and H. Matsuda. 1988. Outward currents through the inwardly rectifying potassium channel of guinea-pig ventricular cells. *Japanese Journal of Physiology.* 38:77–91.

Scheiner, S., and E. A. Hillenbrand. 1985. Modification of pK values caused by change in H-bond geometry. *Proceedings of the National Academy of Sciences, USA.* 82:2741–2745.

Scheiner, S., and J. F. Nagle. 1983. *Ab initio* molecular orbital estimates of charge partitioning between Bjerrum and ionic defects in ice. *Journal of Physical Chemistry.* 87:4267–4272.

Schoenknecht, G., W. Junge, H. Lill, and S. Engelbrecht. 1986. Complete tracking of proton flow in thylakoids—the unit conductance of CF_0 is greater than 10 fS. *FEBS Letters.* 203:289–294.

Schulten, Z., and K. Schulten. 1985. A model for the resistance of the proton channel formed by the proteolipid of ATPase. *European Biophysics Journal.* 11:149–155.

Siczkowski, M., J. E. Davies, and L. L. Ng. 1994. Activity and density of the Na^+-H^+ antiporter in normal and transformed human lymphocytes and fibroblasts. *American Journal of Physiology.* 267:C745–C752.

Silver, M. R., and T. E. DeCoursey. 1990. Intrinsic gating of inward rectifier in bovine pulmonary artery endothelial cells in the presence or absence of internal Mg^{2+}. *Journal of General Physiology.* 96:109–133.

Stoeckenius, W., R. H. Lozier, and R. A. Bogomolni. 1979. Bacteriorhodopsin and the purple membrane of halobacteria. *Biochimica et Biophysica Acta.* 505:215–278.

Thomas, R. C., and R. W. Meech. 1982. Hydrogen ion currents and intracellular pH in depolarized voltage-clamped snail neurones. *Nature.* 299:826–828.

Wagner, R., E. C. Apley, and W. Hanke. 1989. Single channel H^+ currents through reconstituted chloroplast ATP synthase CF_0-CF_1. *EMBO Journal.* 8:2827–2834.

Woolley, G. A., and B. A. Wallace. 1992. Model ion channels: gramicidin and alamethicin. *Journal of Membrane Biology.* 129:109–136.

Zagotta, W. N., T. Hoshi, J. Dittman, and R. W. Aldrich. 1994. *Shaker* potassium channel gating II: transitions in the activation pathway. *Journal of General Physiology.* 103:279–319.